MODIS Optical and Microphysical Properties (MOD06), Atmosphere Level-3 Products (MOD08), and Atmosphere Team Web site

Final Report

January 15, 1992 – January 31, 2004

April 2004

Michael D. King and Steven Platnick
Goddard Space Flight Center, Greenbelt MD

and

G. T. Arnold, J. J. Dinsick, C. K. Gatebe, M. A. Gray, P. A. Hubanks,
E. G. Moody, J. Riédi, B. Wind, G. Wind

Abstract

The Cloud Retrieval Group at Goddard Space Flight Center (GSFC) has been responsible for the following activities:

1. Level-2 algorithm delivery, testing, analysis, and maintenance of the optical and microphysical retrieval component of **MOD06**. The product includes cloud thermodynamic phase, optical thickness, effective particle radius, and integrated water path.

2. The recent design and delivery of an Atmosphere Level-2 Joint Product (**MODATML2**, ~3 MB per daytime granule), containing a subset of MOD35, MOD04, MOD05, MOD06, and MOD07 science data sets, and with spatial subsetting of 1 km data sets.

3. Design, coding, delivery, testing, analysis, and maintenance of the joint Atmospheres Level-3 daily, eight-day, and monthly **MOD08** products.

4. Design and maintenance of the joint **Atmosphere Web Site**, including quicklook imagery and extensive documentation. This undertaking included the development of visualization codes for generating Level-1B true-color quicklook imagery of all daytime observation granules, as well as all operational Level-3 files and daily high-resolution Level-3 files. A visualization code for generating Level-2 quicklooks for a variety of the Atmosphere products is being tested.

5. **Documentation** on behalf of the MODIS Atmosphere team, including the team Validation plan and Quality Assurance plan, as well as contributions to EOS documents.

6. Development and support of the ER-2-based **MODIS Airborne Simulator**

(MAS) used by the Atmosphere team (as well as the broader EOS community) for algorithm development and scientific investigations. This effort has been a joint activity with MODIS personnel at the University of Wisconsin. Instrument maintenance and calibration (since the late '90s) has been the responsibility of the NASA Ames Airborne Sensor Facility, but the Level-1b data analysis software was originally developed by the MODIS cloud retrieval group.

7. **Dissemination of information** to the science community regarding MOD06, MOD08, and the MODIS Atmosphere Team products and activities via numerous conferences and science team meetings. 34 peer reviewed publications have resulted from these efforts, as well as 4 papers submitted or accepted for publication and 4 other publications that include the cloud retrieval algorithm theoretical basis document and MODIS Atmosphere Quality Assurance and Validation Plans.

I. Level-2 Optical and Microphysical Products (MOD06)

A. Summary of Operational Code Through Collection 004

Cloud optical thickness is defined as the vertical integration of extinction over the cloud physical thickness. For water clouds composed of spherical particles, effective particle size is defined as the ratio of the third moment to the second moment of the particle size distribution. The definition of effective particle size for ice clouds is made more difficult because ice particles tend to be nonspherical. For ice clouds, the effective particle size is proportional to the ratio of the total volume to the projected area of the ice particles for a given size and habit distribution.

The simultaneous retrieval of optical thickness and effective particle size derived from cloud reflectance measurements in solar band atmospheric windows is well known (Nakajima and King 1990). MODIS retrievals are performed using a band that is practically non-absorbing for bulk water/ice (0.65, 0.86, or 1.24 μm) combined with three longer wavelength bands where bulk water/ice has significant absorption (1.64, 2.13, and 3.75 μm). Three separate effective sizes are provided in MOD06 corresponding to each of these absorbing bands. The 3.7 μm band includes a significant thermal emission component in addition to the solar reflectance component. The 2.1 μm band retrieval of effective particle size is considered the default value for Level-3 aggregations, which is discussed later in this report. MODIS is the first imager to take measurements in each of these bands simultaneously.

In order to derive cloud optical and microphysical properties from satellite (Terra or Aqua), it is necessary to perform the following steps: (1) identify the probability of a given pixel being cloud contaminated, (2) determine the likely phase of the cloud to be analyzed, and (3) derive the cloud optical and microphysical properties (such as optical thickness, effective radius, cloud top altitude,

etc.).

The MODIS cloud mask algorithm (developed and maintained by Steve Ackerman and Paul Menzel, University of Wisconsin) determines whether a given view of the earth surface is unobstructed by clouds or optically thick aerosol, and whether any clear scene is contaminated by shadow. The algorithm is divided into ten conceptual domains according to surface type (land, water, polar, coastal, and desert) and solar illumination (daytime and nighttime) [cf. Ackerman et al. 1998; King et al. 1998].

Once the cloud mask has been run for all pixels in a scene, it is necessary to interpret the results for application of the cloud retrieval code that follows (see below). The first part of the thermodynamic phase decision tree is focused on identifying whether a cloud mask determination has been obtained for a given pixel and, if so, we check whether the pixel was observed during daytime or nighttime conditions. Next, we read the ecosystem classification bits in the cloud mask to determine which of the five ecosystems the pixel was acquired over. The ecosystem dataset applies to the static ecosystem of land vs. water, and is used for subsequent tests based on whether the ecosystem is ocean, land, snow/ice, coastal, or desert.

Figure 1 shows the cloud mask tests that are run for pixels over ocean surfaces to determine whether the pixel contains clear sky, water cloud, ice cloud, or clouds of undetermined phase. If the scene is classified as cloudy or probably cloudy, then the tests available over ocean surfaces are run individually to estimate the thermodynamic phase of clouds in the scene. As there are limited tests available from the cloud mask, and the thresholds are set, it is possible that ambiguous phase identification still results from these cloud mask results. This was indeed the consequence of this algorithm in the early (collection 3) processing of MODIS data worldwide, in which approximately $1/3$ of the cloudy pixels were identified as water clouds, $1/3$ as ice clouds, and $1/3$ as clouds of undetermined phase (processed as water clouds).

Following the cloud mask phase tests, the current (collection 4) algorithm runs a number of additional tests aimed at increasing the confidence in the cloud thermodynamic phase and reducing the potentially large number of undetermined phase determinations. The first such test is a bispectral threshold algorithm based on the brightness temperature difference between 8.4 and 10.7 μm. This is a simplified and robust modification of the trispectral phase algorithm first described by Strabala et al. (1994), which in turn is based on the difference in optical properties between water droplets and ice crystals, as described by Baum et al. (2000b). This test is run for all cloudy pixels for which the cloud mask tests led to an undetermined phase. Following this test all cloudy pixels are subjected to additional tests of the reflectance ratio between the shortwave bands at 2.1 and 1.6 μm and a visible, nonabsorbing band at 0.66 μm.

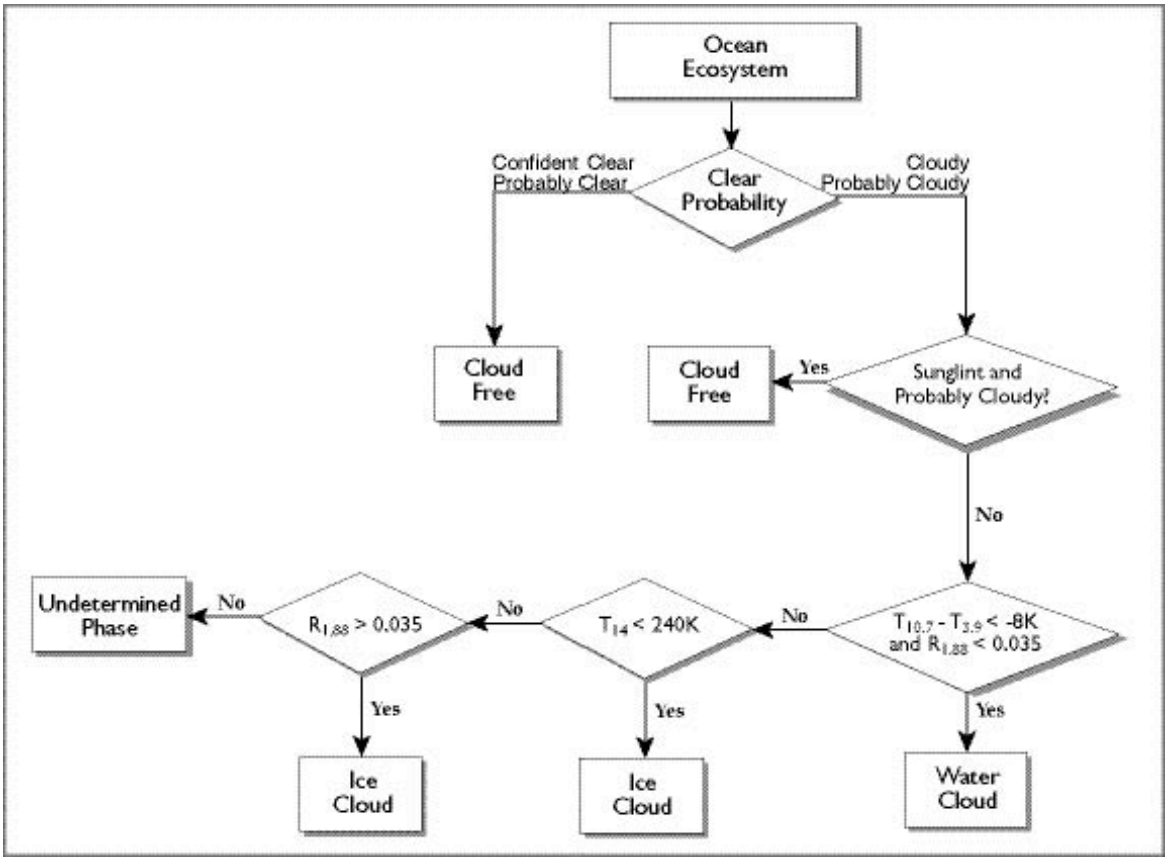

Figure 1. Cloud mask tests for an initial determination of the presence of water clouds, ice clouds, and clear sky over ocean surfaces during the daytime.

Following the identification of the cloudy pixel as water or ice cloud, we next determine the cloud top properties (cloud top pressure and cloud top temperature), an algorithm applied to MODIS data and based on the CO_2 slicing method described by Menzel et al. (2002). Given the cloud top pressure, we estimate the total column precipitable water above the cloud pixel from ancillary input from the NCEP model (and have also done some tests using Goddard's Global Modeling and Assimilation Office model) and estimate the atmospheric transmission for the relevant MODIS bands for all gaseous attenuation above the clouds.

For a strictly absorbing atmosphere, the cloud-top reflectance (i.e., in the absence of an atmosphere) is $R_c = R_{TOA}/t(\mu,\mu_0)$ where R_{TOA} is the measured reflectance at the top of the atmosphere and t is the round-trip or two-way band-averaged transmittance that includes the solar path to cloud top (zenith angle of θ_0) and reflection back towards the satellite (θ). The SWIR/MWIR MODIS bands used in the cloud retrieval algorithm can have appreciable water vapor absorption. Water vapor transmittance in these window bands is primarily dependent on the integrated amount of vapor above-cloud and not on the details of the moisture distribution. In other words, the transmittance function can be approximated as $t(\mu,\mu_0,p_c,w(p_c))$, where w is the above-cloud precipitable water and p_c the cloud-

top pressure. Absorption by trace gases may also be important and will similarly depend on p_c.

A library of band-averaged transmittances was calculated using MODTRAN4 (Berk et al., 1998) for a variety of cloud moisture and temperature profiles, combinations of θ_0 and θ and selected pressure heights. Mean transmittances and standard deviations for the profiles were catalogued. Typically, the dispersion was on the order of a few percent or less making such a library suitable for cloud retrieval atmospheric corrections. In the cloud retrieval algorithm, the transmittance library is used in conjunction with the MODIS cloud-top pressure product and integrated water amounts calculated from NCEP GDAS. For the 0.65 μm band (only used for clouds over land), Rayleigh scattering can be important modifier of radiation for thin clouds and for thick clouds at large solar and viewing angles. A Rayleigh correction for this band for this band is implemented using an iterative method (Wang and King, 1997) that is applied after the absorption correction.

Two-way spectral transmittances for an example Terra granule off Peru are shown in Figure 2 (unmapped projection) along with the above-cloud column water and cloud-top pressure fields. Absorption in the 0.65 μm band is primarily a result of relatively uniform stratospheric ozone; view angle (swath-symmetric) and solar zenith angle variations are seen. All other bands have appreciable water vapor absorption that increases with band central-wavelength. The result is a transmittance pattern that is a function of cloud height and modeled moisture profiles as well as geometry. Note that in some areas of the stratocumulus, the 2.1 μm transmittance can be as low as ~0.9 which means correcting the measured satellite reflectance by the factor 0.90^{-1} (> 10% increase).

After having corrected the upwelling radiance from the cloudy pixels by transmission losses above the cloud, the next step is to estimate the surface reflectance below the cloud at the six MODIS bands used in the cloud optical property retrieval. For collection 4 processing, we use the IGBP land cover classification scheme at 1 km resolution globally (data product MOD12Q1) and derive relationships between the 'white sky' (diffuse) albedo derived from MODIS atmospherically corrected spectral radiances on a 16 day time period (data product MOD43B3).

Figure 3 shows the white sky albedo map for global land surfaces at 1.64 μm for July 2001 (based on collection 3 data). At the present time (collection 4), these high resolution albedo data are related to ecosystem, which is used as a proxy, and we use a sinusoidal variation of albedo over the 12 month season with no seasonal variation in the tropical belt between 20°N and 20°S but a sinusoidal seasonal cycle poleward of 30° in both hemispheres. These surface spectral albedos will be replaced in collection 5 processing with a seasonal filled-in surface albedo data product, described by Moody et al. (2004).

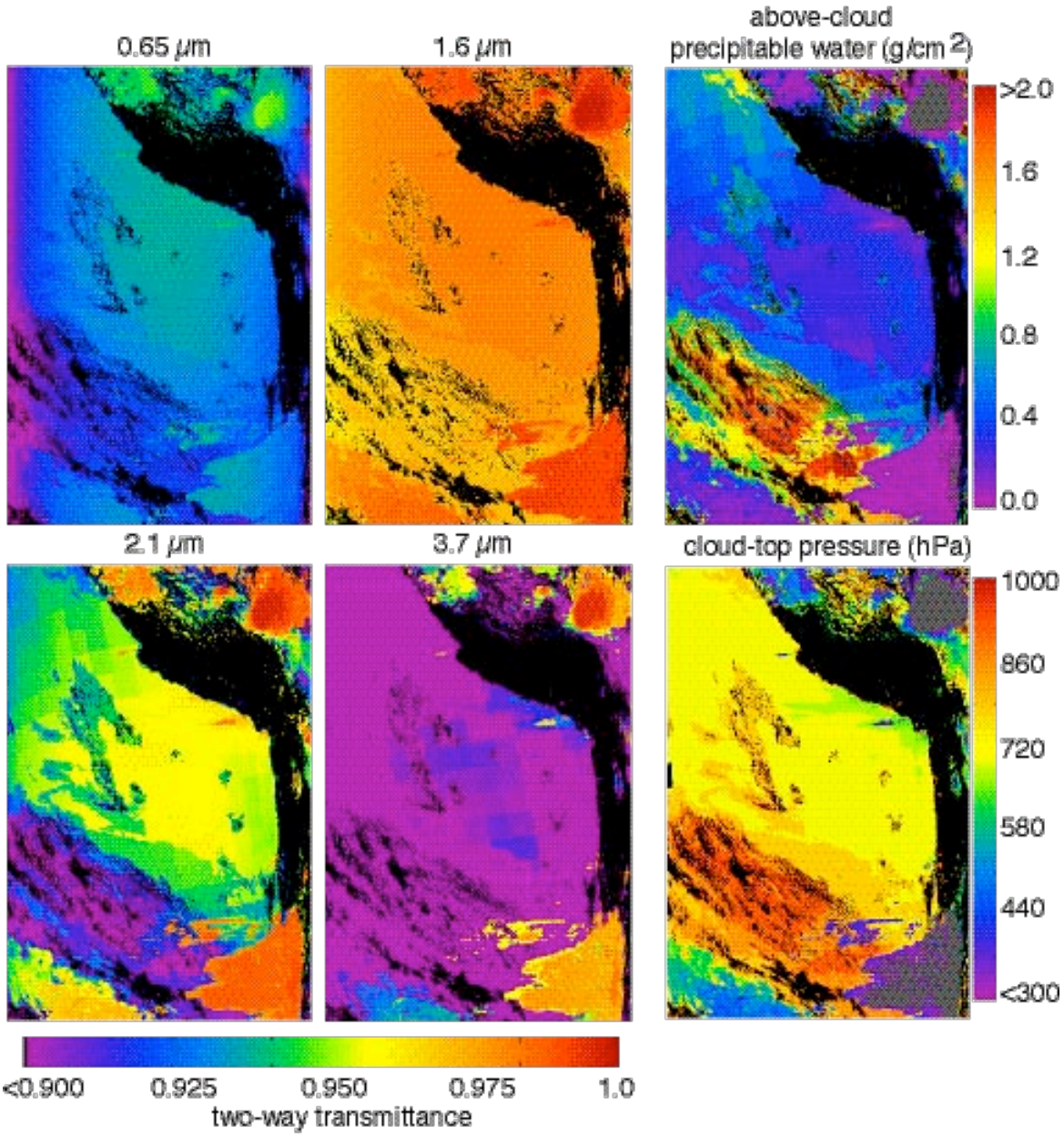

Figure 2. Two-way band-averaged transmittance for four MODIS bands used in the optical/microphysical retrievals (set of four panels to the left). The transmittance routine requires the integrated above-cloud water amount (upper right panel), which is, in turn, derived from model moisture profile data and the cloud-top pressure field (lower right).

Having determined the underlying surface albedo at the corresponding MODIS bands under cloudy sky conditions, the cloud retrieval algorithm described by Nakajima and King (1990) is applied to these data, where we have made use of different table look-up libraries for liquid water and ice cloud reflectance based on the thermodynamic phase identified for the cloudy pixel. These light scattering properties for ice crystals with different sizes and habits were performed by Ping Yang based on a combination of the improved geometric optics method

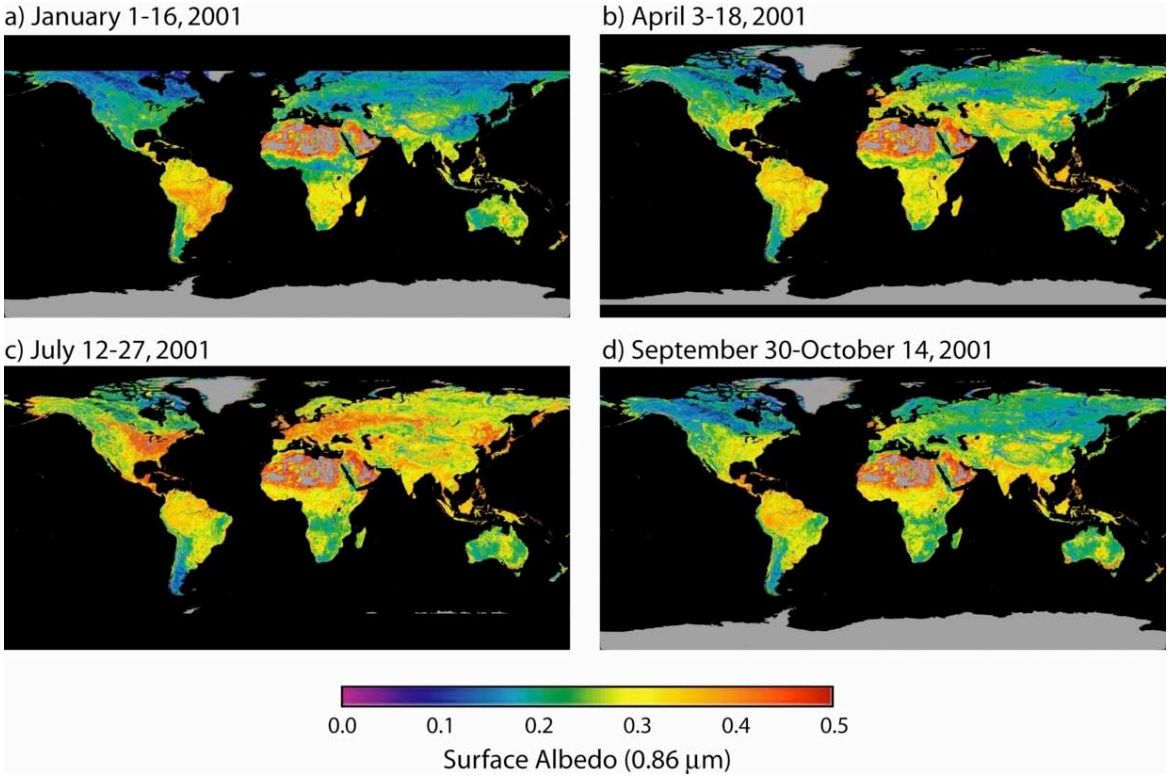

Figure 3. Spatially complete white sky albedo at 0.86 μm for for the 16-day periods of (a) January 1-16, (b) April 3-18, (c) July 12-27, and (d) September 30-October 14, 2001 (Moody et al. 2004).

(GOM2) and the finite different time domain (FDTD) technique (*Yang and Liou*, 1996a,b). FDTD is applied to size parameter smaller than 20 whereas GOM2 is employed for size parameters larger than 20. The remote sensing retrievals are based on library calculations of plane parallel homogeneous clouds overlying a black surface in the absence of an atmosphere. Separate libraries have been built for water and ice clouds; currently no separate library exists for mixed phase clouds. The bulk scattering properties for the ice clouds used by Ping Yang are based on mixtures of hexagonal plates, columns, bullet rosettes, and aggregates (Baum et al. 2000a) and a set of particle size distributions developed from mid-latitude cirrus field campaigns.

Figure 4 shows an example of the cloud optical thickness and effective radius retrievals using collection 4 algorithms for a daytime granule of Terra-MODIS data over the Western Pacific Ocean near the Kamchatka Peninsula on 10 August 2001 at 00:25 UTC (King et al. 2003a). The cloud optical thickness image in (a) shows extensive cloud cover over the Sea of Okhotsk, including mid-level and upper-level ice clouds, whereas the Bering Sea to the east of the Peninsula contains extensive marine stratocumulus clouds with numerous ship tracks in the south-eastern portion of the image. The optically thick marine stratocumulus to the east of the Peninsula are identified as water clouds with optical thicknesses $\tau_c(0.65\ \mu m)$ up to ~25. The optically thick ice clouds over the Sea of Okhotsk and around the southern portion of the Kamchatka Peninsula have cloud optical

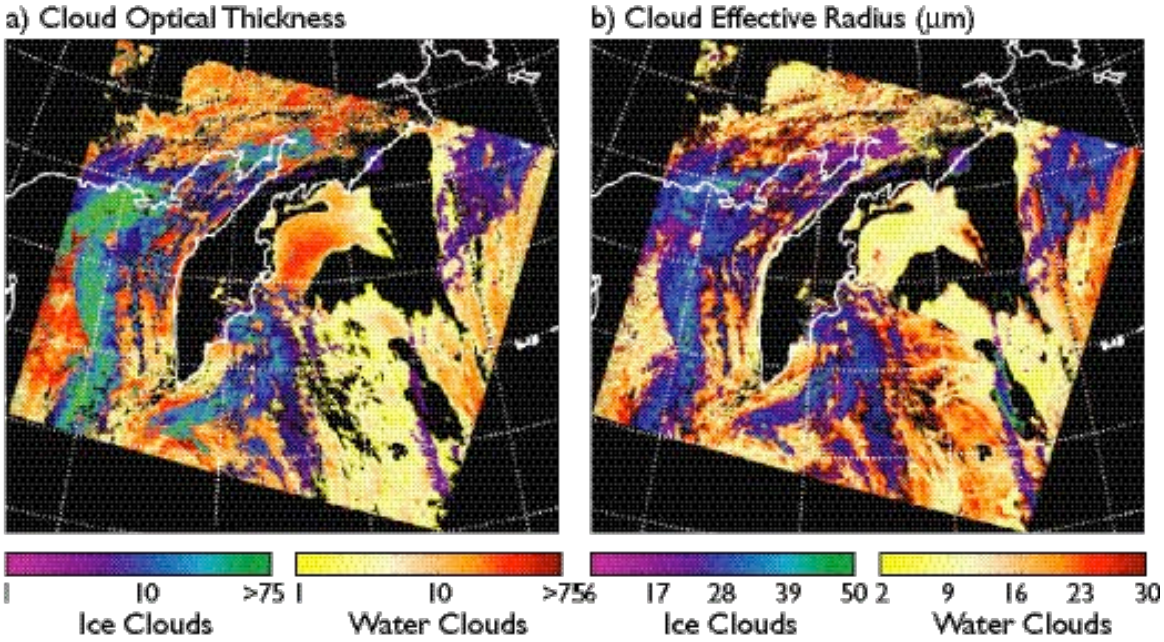

Figure 4. Cloud properties over the western Pacific Ocean off the Kamchatka Peninsula on August 10, 2001, based on Terra/MODIS data. Panel (a) is the cloud optical thickness of one MODIS granule, showing marine stratocumulus clouds with ship tracks as well as upper level ice clouds. Panel (d) shows the cloud effective radius derived from all cloudy pixels, where we have used a separate color bar to denote clouds processed as ice and water clouds (King et al. 2003a).

thicknesses approaching 40. The ship tracks are not easily identified in the cloud optical thickness image shown here, but they result in reduced effective radii in the microphysical retrievals shown in (b). Finally, the cloud top pressure for the cloud-filled pixels(not shown here), show that the water clouds lie predominantly between 700 and 850 hPa, whereas the optically thick ice clouds over the Sea of Okhotsk lie at altitudes above the 500 hPa level.

For operational processing, snow and ice cover is provided by the NISE product; when snow or ice is present, and spectral albedos are provided from field measurements. Further details regarding the MODIS optical and microphysical retrieval algorithm are described in Platnick et al. (2003).

Table 1 summarizes the cloud optical properties algorithm as currently run in

TABLE 1. MOD06 Cloud Optical Properties Software

Software Module	Source Lines	Comments	Total
Science algorithm (computation and phase determination)	3,032	1,988	5,020
Ancillary package (water vapor, temperature, surface albedo, etc.)	3,925	3,907	7,832
System code (data input/output, QA, metadata, etc.)	2,385	2,014	4,399
Total	**9,342**	**7,909**	**17,251**

TABLE 2. Pending Cloud Optical Properties Enhancements and Improvements

Pending Software Enhancements and Improvements
Add a 1.6 μm vs. 2.1/3.7 μm retrieval algorithm for liquid water clouds over snow and sea ice surfaces (Terra only), as described by Platnick et al. (2001)
Improve the ice crystal models used in the global retrieval algorithm based in part on CRYSTAL-FACE and other in situ datasets
Improve and examine multi-layer cloud detection and retrievals
Implement improved seasonal and spectral surface albedo maps based on an annual model that incorporates greenup, maturity, senescence, and dormancy cycles of terrestrial vegetation
Improve and otherwise enhance uncertainty and QA analysis, based in part on model sensitivities and view angle dependencies

production. It is part of PGE06 and the output field is stored as part of data product MOD06 (Terra) and MYD06 (Aqua). Of the 9,342 lines of science source code, approximately half are written in Fortran 77 and the other half in Fortran 90. At the end of this contract period, the entire algorithm had been rewritten in Fortran 90 which is both more efficient, easier to maintain, and faster. This Fortran 90 version will be inserted into production, along with additional science updates, for collection 5 processing in late summer 2004.

Although considerable improvements have been made in the science accuracy, reliability, and phase discrimination routines in this very sophisticated software program generation executive, Table 2 summarizes science items still remaining for future enhancements and improvements in the foreseeable future.

There are currently three inferences of cloud phase found in the MOD06 cloud product: a bispectral IR algorithm stored as a separate Science Data Set (SDS) and a decision tree algorithm that includes cloud mask results as well as the IR and SWIR tests. The latter phase retrieval is stored in the MODIS "Quality_Assurance_1km" output SDS and not as an individual SDS, a fact that has caused some confusion among users of this product. The decision tree algorithm gives the phase that was used in the subsequent optical and microphysical retrieval. The current IR phase algorithm is at a 5 km spatial resolution, while the other two are at 1 km. In collection 5, a 1 km SDS with the phase determination used in the cloud optical properties algorithm will be explicitly included in the output file to reduce community misinterpretation of results.

B. Research Activities and Collection 005 Efforts

A number of research activities are being targeted for collection 005 deliveries in summer 2004. A brief summary of these efforts is given below.

1. Improved Spectral Surface Albedo Maps and Value-added Albedo Products

As previously mentioned, the optical and microphysical retrieval algorithm requires surface albedo in visible and SWIR bands as the boundary condition for cloud radiative transfer modeling over land. Previously, a single 16-day com-

posite of spectral albedo from the operational MOD43 product was available, requiring questionable assumptions on seasonal changes. A year's worth of MOD43 16-day spectral albedo composites have been archived in the GES DAAC since the last major optical and microphysical algorithm software delivery. With these data, a complete yearly surface spectral albedo map is now available for use in the next production collection (cf. Figure 3). Cloud and seasonal snow cover, however, curtail retrievals to approximately half the global land surfaces on an annual equal-angle basis, precluding MOD43 albedo products from direct assimilation into the optical and microphysical production environment.

A temporal interpolation technique has been developed to fill missing data in the operational albedo product by imposing pixel-level and local regional ecosystem-dependent phenological behavior onto retrieved pixel temporal data in such a way as to maintain pixel-level spatial and spectral detail (Moody et al., 2004). The resulting value-added product provides spatially complete surface albedo maps and statistics for both direct and diffuse illuminations. Data are stored on one-minute and coarser resolution equal-angle grids for the first seven MODIS wavelengths (0.47 μm through 2.13 μm) and for three broadband wavelengths (0.3-0.7 μm, 0.3-5.0 μm and 0.7-5.0 μm).

2. Quantitative Estimation of Pixel-level Uncertainties

A methodology for assessing pixel level uncertainty for cloud optical thickness and effective particle radius has been developed and is in the process of being tested on global MODIS data. The uncertainties are based on chain rule (Jacobian) derivative calculations using existing cloud reflectance libraries. While limited to plane-parallel clouds (i.e., 3-D cloud geometry uncertainty is not assessed), it does provide a base uncertainty. To date, components of the uncertainty include instrument calibration, atmospheric corrections, and surface spectral albedo maps. An example is shown in Fig. 5.

3. Multilayer/phase Cloud Detection

An algorithm for detecting multi-layer and multi-phase cloudy pixels was developed and tested over a variety of surfaces (land, ocean, sea ice, snow); assessment for use in collection 5 is ongoing. The algorithm has two parts. First, it determines above-cloud precipitable water (PW) differences between the operational MOD06 method (using cloud top pressure heights and GDAS profiles) and a 0.94 μm algorithm developed for determining above-cloud column water vapor amount; the difference is normalized by the column PW as given by GDAS and a threshold is chosen. A large normalized PW difference indicates a multilayer/phase situation (cirrus overlying a water cloud) where the MOD06 optical/microphysical retrieval algorithm chose to treat the scene as if it were composed of a single layer ice cloud, but where a water cloud signal is likely a significant component to the VIS/SWIR bands used for the MOD06 retrievals. A second test looks at disagreements between the MOD06 bi-spectral IR cloud phase algorithm (8.5 and 11 μm) and the chosen phase for the retrieval (includes

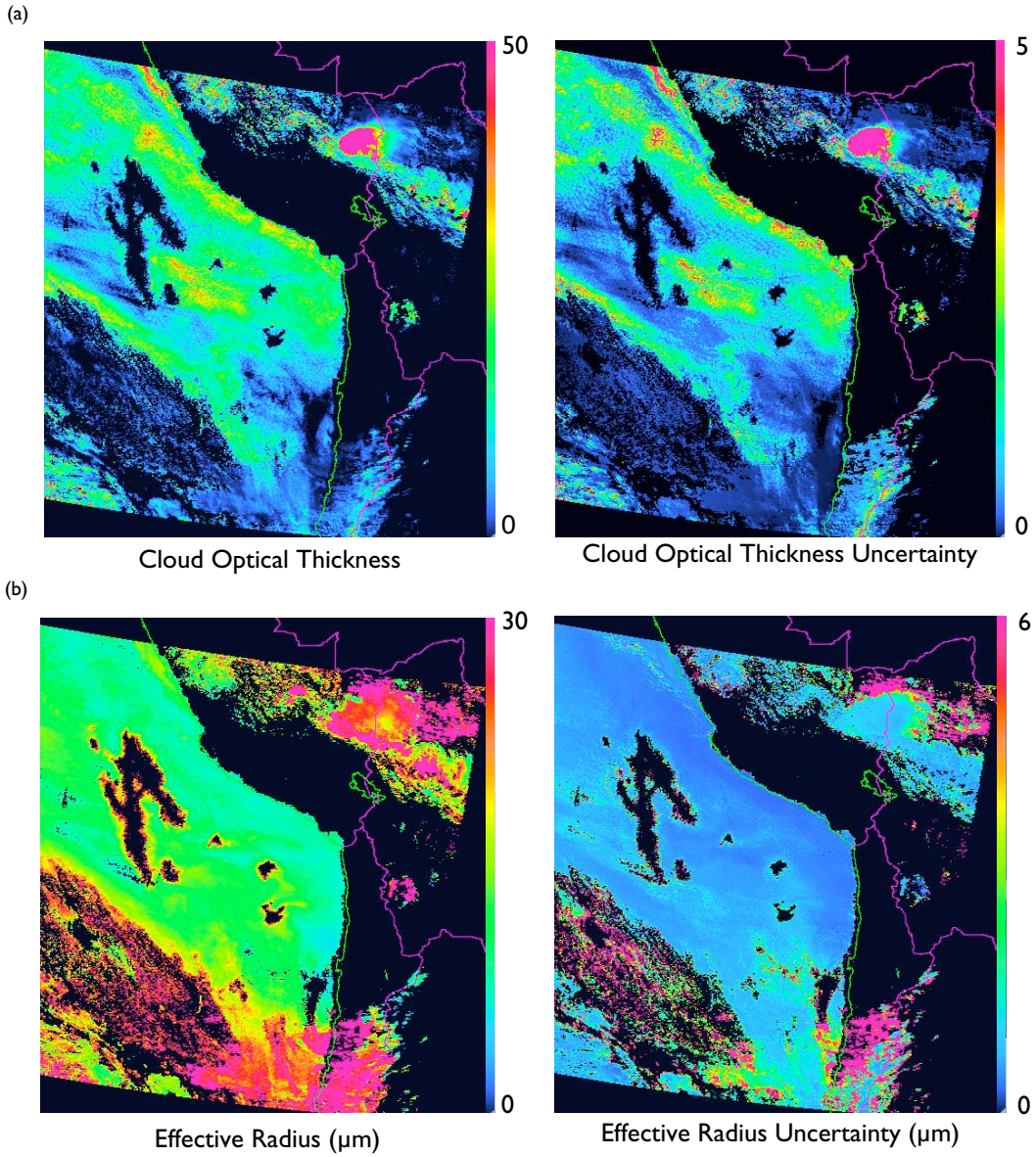

Figure 5. Cloud optical thickness (τ) and uncertainty in τ, and (b) effective radius (r_e) and uncertainty in r_e, for a MODIS Terra granule off the coast of Peru and Chile on July 18, 2001.

SWIR tests and cloud mask test results). A disagreement typically indicates a multi-layer cloud situation where the MOD06 retrieved the scene as if it was composed of a single layer water cloud, but where IR bands detected an ice cloud signature. The multi-layer/phase detection method doesn't require additional radiative transfer libraries. An example image is shown in Fig. 6.

C. Level-2 Lessons Learned

- The global cloud optical properties retrieval algorithm developed from experience based on multispectral airborne datasets over selected environmental conditions, and AVHRR-based experience using somewhat different, and

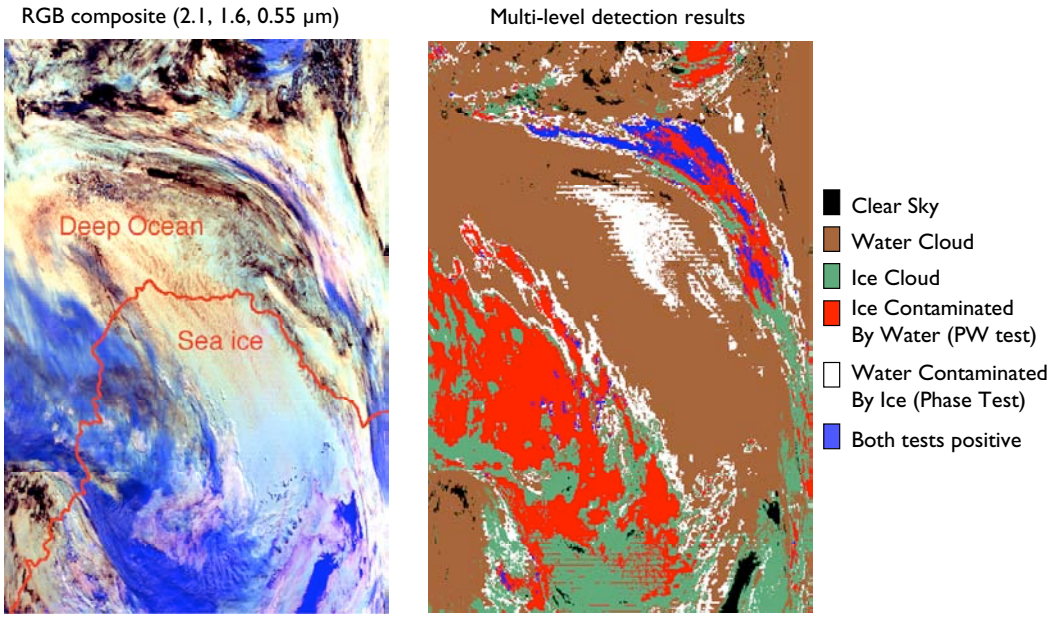

Figure 6. Example pixel-level multi-level/phase detection results for MODIS Terra, November 20, 2002, for a granule in the Antarctic Ocean. The boundary between open ocean and sea ice is indicated in the RGB composite (left panel). A positive multilevel cloud result (right panel) is indicated by red, white, or blue colors (see color bar for details); results appear insensitive to the presence of sea ice.

spectrally much broader, bands. Adapting these concepts and experiences to a robust global analysis system was exceedingly challenging.

- Extensive experience from field experiments in the Arctic ocean and nearby tundra of northern Alaska led to adapting a 1.24 μm band to the cloud optical thickness over snow and sea ice surfaces to enhance contrast. This had never been done before. Further work using the 1.6 and 2.1 μm bands for simultaneous retrieval of cloud optical thickness and effective radius over snow and sea ice surfaces developed from airborne MAS observations (Platnick et al. 2001, King et al. 2004) shows promise, but has not yet been incorporated into global processing. This has also never been done before, and is most encouraging.

- Development of a Rayleigh correction algorithm over ocean surfaces is new, and subtle, and appears to work beneficially. This came about through airborne field campaign observations with the MAS.

- Software requirements and standards, including metadata, QA, HDF-EOS, and the like led to considerable angst and development starts and restarts, but ended up providing a very robust processing environment.

- Continuity in integration software team was crucial, and the long-term involvement of Rich Hucek on the MODIS Data Support Team to interface with the production system and integrate software into production was exceed-

ingly valuable. Furthermore, when the MODIS Adaptive Processing System (MODAPS) incorporated Linux clusters into the production environment, in addition to SGI workstations, SDST, and especially Rich Hucek, ported the SGI-based software to work flawlessly under Linux. The development team could not test this, since this team possessed no Linux workstations.

- Visualization tools to diagnose processing paths (water, ice clouds, surface types, Rayleigh tests, atmospheric correction, etc.) enabled ready diagnosis of conditions under which the algorithm was operating as designed, and conditions that required further analysis.

II. Level-2 Joint Atmosphere Product (MODATML2)

The post-launch MODIS Atmosphere Level 2 Joint Product contains a subset of key parameters taken from the standard at-launch Level-2 products: Aerosol, Water Vapor, Cloud, Profile, and Cloud Mask. The new Joint Atmosphere product was designed to be small enough to minimize data transfer and storage requirements, yet robust enough to be useful to a significant number of MODIS data users. Scientific data sets (SDSs) contained within the Joint Atmosphere product cover a full set of high-interest parameters produced by the MODIS Atmosphere team, and are stored at 5 km and 10 km (at nadir) spatial resolutions. There are two MODIS L2 Joint Atmosphere data product files: MODATML2, containing data collected from the Terra platform; and MYDATML2, containing data collected from the Aqua platform. Both of these products began production on October 14th 2003. The first available data are for day 285 (October 12, 2003) for Aqua and day 286 (October 13, 2003) for Terra.

A few limitations were introduced into the Joint Product to reduce the file size. First, some parameters that were stored at 1-km resolution in their original (source) Level 2 product file were subsampled to 5 km in the Joint product. These include the cloud mask, cloud optical thickness, cloud effective radius, cloud quality assurance (includes cloud phase information), cirrus reflectance, and the precipitable water (near IR) parameters. Second, geolocation arrays that were stored as 4-byte floating-point real numbers in the original (source) product file were compressed to 2-byte scaled integers (sacrificing only 0.001° of geolocation accuracy). Finally, only a limited set of Quality Assurance (QA) arrays were included, and only for parameters where they were absolutely crucial for data use/interpretation. These drawbacks were considered acceptable in the context of the overall goal of this project: to create a small and user-friendly Level 2 HDF file of key MODIS Atmosphere SDSs such that a full day of data could be stored on a CD (< 700 MB).

Table 3 summarizes the Science Data Sets (SDSs) contained in the Level-2 Joint Atmosphere Product, which consists of SDSs at a resolution of 5 km for many data sets and 10 km for the aerosol data sets. With this design, 144 daytime granules, defined as a 5 minute, or 2300 x 2000 km section of data, would be approximately 2.7 MB each, with each of the 144 nighttime granules being 1.1 MB.

TABLE 3. Science Data Sets of the new MODIS Level-2 Joint Atmosphere Product

	SDS Size (kB)	
Science Data Set	Daytime	Nighttime
Global Attributes	75	75
Cloud mask (1st byte)	109	109
Cloud optical thickness	219	
Cloud effective radius	219	
Cloud top pressure	219	219
Cloud phase daytime	109	
Cirrus reflectance	219	
Cloud quality assurance (optical properties)	109	
Precipitable water (near infrared clear sky)	219	
Precipitable water (thermal infrared)	219	219
Latitude (5 km)	219	219
Longitude (5 km)	219	219
Aerosol optical thickness	54	
Aerosol optical thickness ratio (fine mode to total)	54	
Aerosol solution index for small particles (ocean)	54	
Aerosol solution index for large particles (ocean)	54	
Aerosol quality assurance	54	
Latitude (10 km)	54	
Longitude (10 km)	54	
Solar zenith angle (10 km)	54	
Zenith angle (10 km)	54	
Relative azimuth angle (10 km)	54	
Total size (kB)	**2694**	**1060**

With this design, a whole day's worth of data would be no larger than ~528 MB and could fit on a CD for easy distribution.

Figure 8 shows a visualization of effective radius of all water and ice clouds retrieved for October 28, 2003 based on Terra/MODIS observations. The vertical scale is based on the cloud top pressure and is used to stretch the height of the clouds. The transparency is based on cloud optical thickness, and the colors are the effective radius of water and ice clouds separately. Note that the water clouds tend to be low in altitude whereas the ice clouds are higher in the atmosphere. This visualization is a perspective from the Pacific Ocean with Australia identified in the lower left portion of the image.

III. Level-3 Joint Atmosphere Products (MOD08)

A. Overview

There are six Level-3 atmosphere products covering three time intervals (daily, eight-day, and monthly) and two instrument platforms (Terra and Aqua). The *Earth science data type* (ESDT) name, used as the *hierarchical data format* (HDF) filename prefix for each product, is derived from the source platform (*MOD08* for Terra and *MYD08* for Aqua) and time interval (*D3* for daily, *E3* for eight-day, and *M3* for monthly).

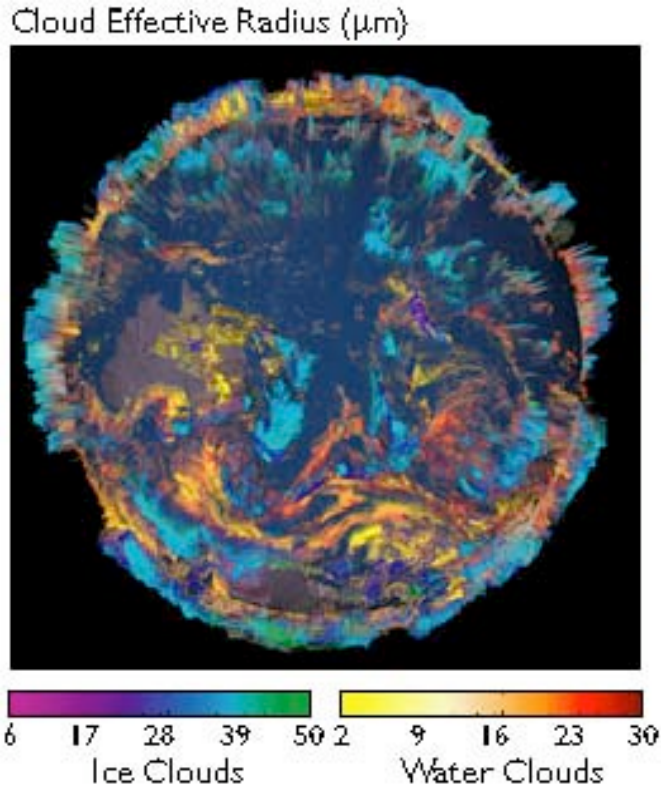

Figure 7. Cloud effective radius derived from the daily joint atmosphere product on October 28, 2003, based on Terra/MODIS data. Cloud top pressure is used to scale the vertical extent of the clouds, transparency to delineate cloud optical thickness, and the color bars to denote the effective radius of ice clouds and water clouds separately (based on visualization by Reto Stöckli).

These Level-3 products contain statistics derived from four Level-2 atmosphere products: aerosol, precipitable water, cloud, and atmospheric profiles. The daily Level-3 product contains roughly 600 statistical datasets that are derived from approximately 80 scientific parameters from the four Level-2 products noted above. The 8-day and monthly Level-3 products are somewhat larger in size than the daily product, comprising roughly 800 statistical datasets.

Statistics are sorted into 1° grid boxes on an equal-angle global projection. The set of statistics computed for each parameter depends on the parameter being considered, and might include: simple statistics (mean, minimum, maximum, standard deviation), parameters of normal and log-normal distributions, fraction of pixels that satisfy general cloud conditions (e.g., cloudy or clear), histograms of the distribution within each grid box, histograms of the confidence placed in each measurement, and histograms and/or regressions derived from comparing one science parameter to another. Any of the Level-3 statistics noted above may be computed for a subset of Level-2 pixels that satisfy some condition (e.g., liquid water or ice clouds). Level-3 statistics are computed by sub-sampling Level-2 data at the resolution of the internal Level-2 (input file) geolocation. This sub-

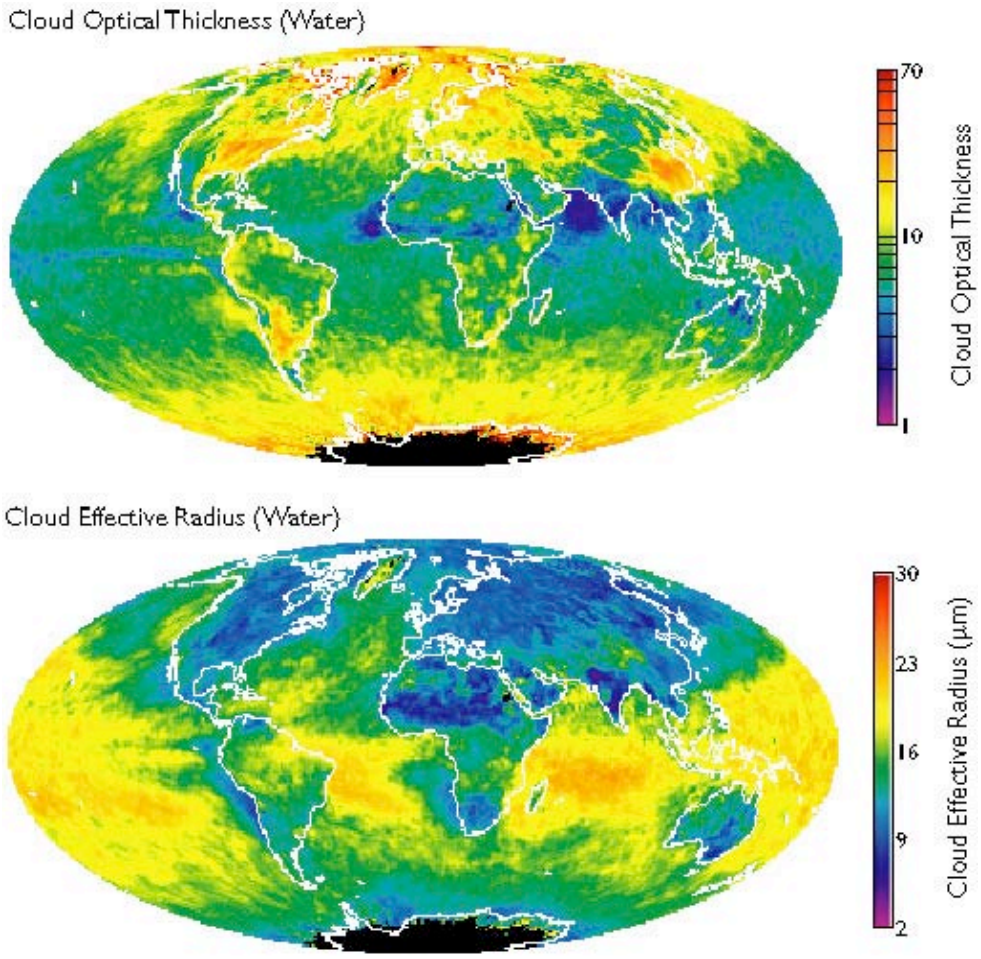

Figure 8. Global distribution of cloud optical thickness (upper panel) and effective radius (lower panel) of liquid water clouds derived from MODIS measurements on the Terra platform for April 2003. These results represent the QA-weighted (most confident solutions weighted more heavily).

sampling only impacts the few Level-2 parameters that have their data stored on a grid that is finer than the stored geolocation (cirrus detection and cloud optical properties only).

Figure 8 shows monthly mean values of cloud optical thickness and effective radius of liquid water clouds for April 2003, derived from MODIS observations on the Terra satellite. The cloud optical thickness is lower in the Intertropical Convergence Zone because clouds in this region are invariably topped by ice clouds and are hence retrieved as ice cloud properties. The effective radius, shown in the lower pane of Fig. 8, is noticeably larger in the southern Hemisphere than the Northern Hemisphere, and also larger over the oceans than the land, reflecting, at least in part, the larger concentration of aerosol particles over the land that lead to larger numbers of smaller drops than maritime clouds.

Figure 9 shows a joint histogram of cloud optical thickness and effective radius derived from the MODIS Level-3 joint atmosphere product for June 2003 for a

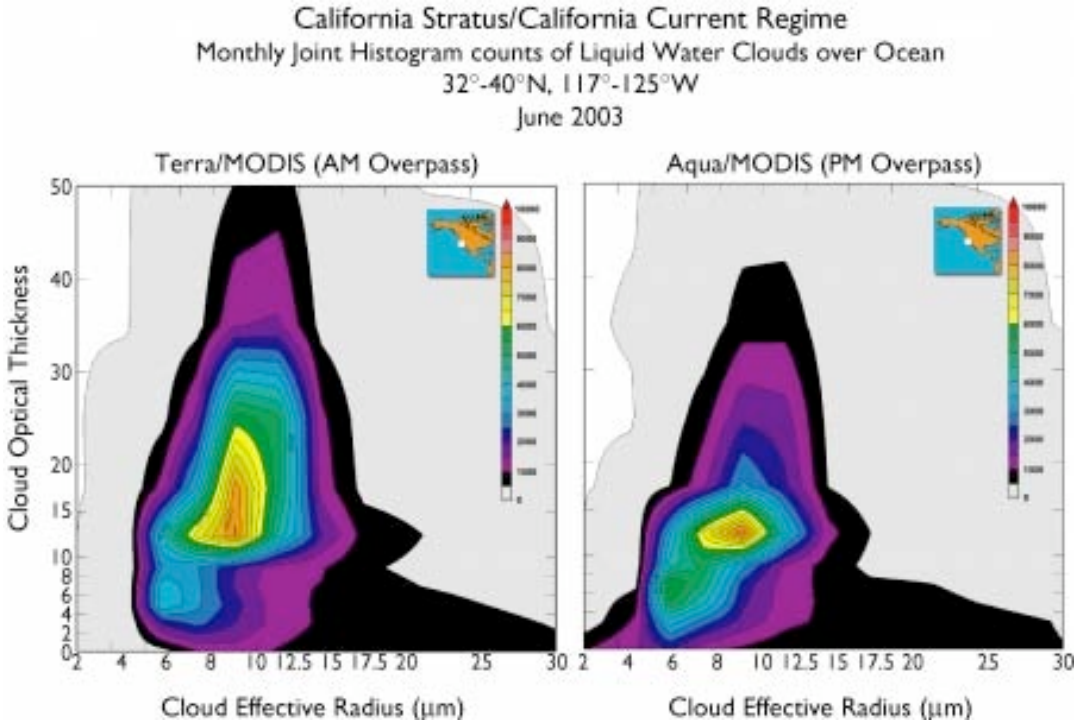

Figure 9. Histogram of the joint probability of cloud optical thickness and effective radius derived from the Level-3 joint atmosphere product for June 200e for a region off the coast of California bounded by 32°-40°N and 117°-125°W. All liquid water cloud retrievals over ocean in this latitude-longitude box have been aggregated. The grid pattern reflects the bin boundaries in this Level-3 data product.

region off the coast of California bounded by 32°-40°N and 117°-125°W. All liquid water cloud retrievals over ocean in this latitude-longitude box have been aggregated, and the grid pattern reflects the bin boundaries in this Level-3 data product.

The joint histogram on the left was obtained from Terra/MODIS observations in the morning (around 10:30 AM local time) and the histogram on the right was obtained from Aqua/MODIS observations in the afternoon (around 1:30 PM local time). As is common for marine stratocumulus clouds, they are optically thicker and hence brighter in the morning, burning off and decreasing in water content in the early afternoon. The mode optical thickness of these boundary layer clouds was around 15 in the morning and perhaps 12 in the afternoon, but there are more optically thick clouds present in the morning.

The effective droplet radius was not much different in the morning than the afternoon, being around 9 μm in both cases. This is characteristic of marine stratocumulus clouds in other regions of the world (e.g., Namibia/Angola and Peru) where the droplet size is not much different in the morning from the afternoon.

Joint histograms and marginal probability density functions are new with MODIS, and have never been constructed in prior satellite projects. They are hence of great relevance to studies of global climate and of value to climate

TABLE 4. MOD08 Level-3 Joint Atmosphere Product Software

Process	Products	Source Lines (language)	File Spec Input Lines (language)	Com-ments	Total Lines
Low-Res Tile	5° latitude tile pre-processor	21,819	10,354	5,040	37,213
Low-Res Daily	MOD08_D3 MYD08_D3	18,899	10,366	1,000	30,265
Low-Res Eight-day	MOD08_E3 MYD08_E3	26,947	14,519	3,397	44,863
Low-Res Monthly	MOD08_M3 MYD08_M3	26,947	14,519	3,397	44,863
High-Res Tile	5° latitude tile pre-processor	12,517	4,598	5,461	22,576
High-Res Daily	MOD08D3H MYD08D3H	4,343	1,319	1,196	6,858
Total		**111,472**	**55,675**	**19,492**	**186,639**

model investigations.

Table 4 summarizes the Level-3 atmosphere algorithm software as currently run in production. These algorithms are executed in *program executable* (PGE) 69 and 56 (tile and daily for both low and high-resolution), PGE70 (eight-day), and PGE57 (monthly). Of the 111,472 lines of Level-3 source code, approximately 60% are written in Fortran 90 and 40% are written in Fortran 77. The 55,675 lines of Level-3 file specs are written in the Common Data Language (CDL) format.

The MODIS Atmosphere Level-3 software was cleverly designed to be flexible enough to handle the varied and complex HDF product requirements, yet streamlined enough to minimize the potential error frequency and maintenance requirements.

Statistics are sorted into 1° x 1° cells on an equal-angle grid that spans a 24-hour (0000 to 2400 UTC) interval and then summarized over the globe. It should be noted that browse images are available in both the native equal-angle (lat-lon) grid as well as an equal-area (Hammer-Aitoff) grid. A high-resolution (0.1° grid) daily code of selected Atmosphere Level-2 SDSs is run in the operational environment; quicklook imagery is posted to the MODIS Atmosphere Web site but the file is not archived. An overview paper on the collection 4 MODIS Atmosphere's Level-3 products was published in the TGRS Aqua special issue (King et al. 2003a).

B. Level-3 Lessons Learned

- The development of the Level-3 algorithm was never proposed, but accepted as additional duties during the MODIS contract period. Its development started at the end of 1996 for a Terra launch 3 years hence. The original brainstorm of this algorithm was the design element that required that no

computations be done in this code, that everything had to be done in Level-2, and the output was dictated largely by the file spec. Any change in the file spec would propagate directly into Level-3 aggregation. The development team consisted of 2 post-docs and one scientific programmer (Paul Hubanks), who also developed and maintains the MODIS-Atmosphere Web Site (see below). Because of the sophisticated nature of its design, these codes can now be maintained with one person only.

- Level-3 products and visualizations are valuable to the Science Team and outside community for evaluating the quality and content of their algorithms.

- A design that put all atmosphere products into a single Level-3 file, and could be run from granules in zones, made the production environment very efficient and had very low operational memory overhead (in contrast to the MODIS Land and Ocean designs).

IV. MODIS Atmosphere Web Site

A. Overview

The MODIS atmosphere web site modis-atmos.gsfc.nasa.gov contains a wealth of information for the user of MODIS data. This information includes:

- ❑ Images
  - ➢ Level-1b daytime granules for all Terra and Aqua scenes
  - ➢ Level-3 daily, eight-day, and monthly images
  - ➢ Level-2 atmosphere images for every daytime granule on selected 'golden days'
- ❑ Validation activities and links
- ❑ References
  - ➢ Presentations (PowerPoint, with movies)
  - ➢ Publications (pdf)
  - ➢ Algorithm Theoretical Basis Documents (ATBDs)
  - ➢ Validation and Quality Assurance Plans
- ❑ Tools
  - ➢ Granule locator tools
  - ➢ Spatial and dataset subsetting
  - ➢ Visualization and analysis
- ❑ Data product information
  - ➢ Data availability calendar
  - ➢ PGE modification history and known problems
  - ➢ Format and content
  - ➢ Grids and mapping
  - ➢ Acquiring data

Table 5 shows the number of images and image volume produced and posted to the Web site every day for both Terra and Aqua data using automated perl

TABLE 5. MODIS Atmosphere Web Site Image Production

	Number of Images	Image Volume (MB)
Terra		
Level-1B	340/day	43
Level-3 Daily	1600/day	39
Level-3 Eight-day	2200/eight-days	64
Level-3 Monthly	2200/month	64
Level-3 Daily (high resolution)	32/day	22
Aqua		
Level-1B	340/day	43
Level-3 Daily	1600/day	39
Level-3 Eight-day	2200/eight-days	64
Level-3 Monthly	2200/month	64
Level-3 Daily (high resolution)	32/day	22
Total (per day)	***4641***	***228***

scripts.

Figure 10 shows a screen shot of the Level-1b true color images page for Terra on March 29, 2004. From this screen a user can click on one of the maps to determine what 5 min UTC time the Terra satellite was over a region of interest, and

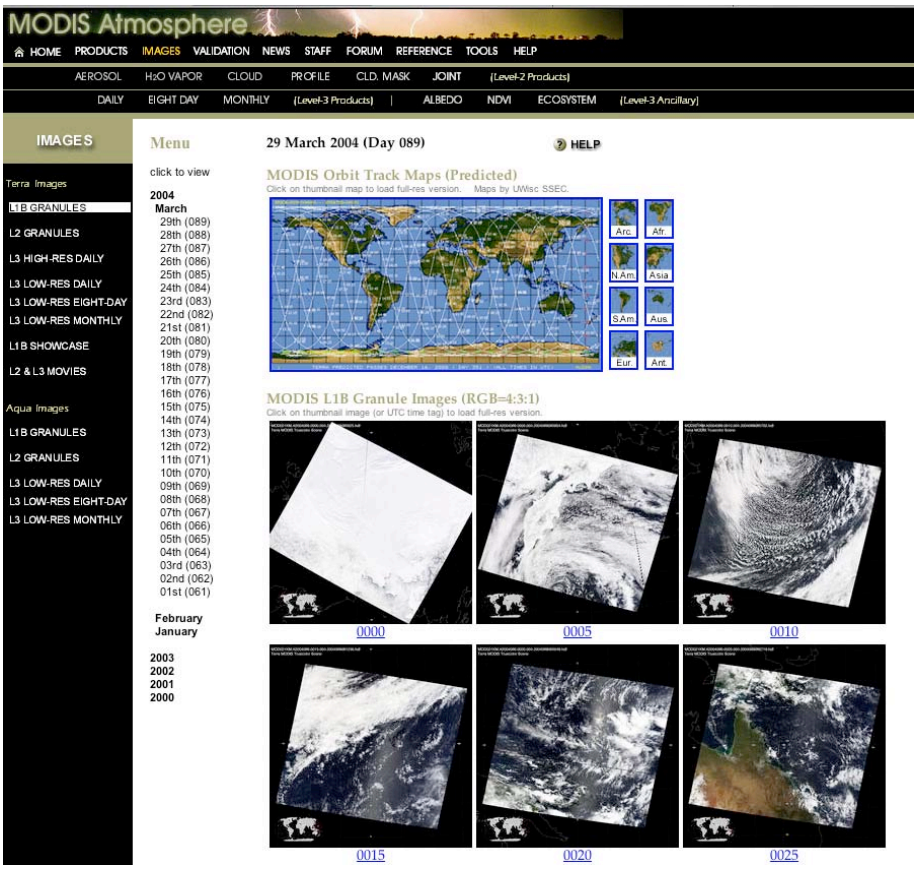

Figure 10. Level-1b true color images of every daytime granule for Terra on March 29, 2004.

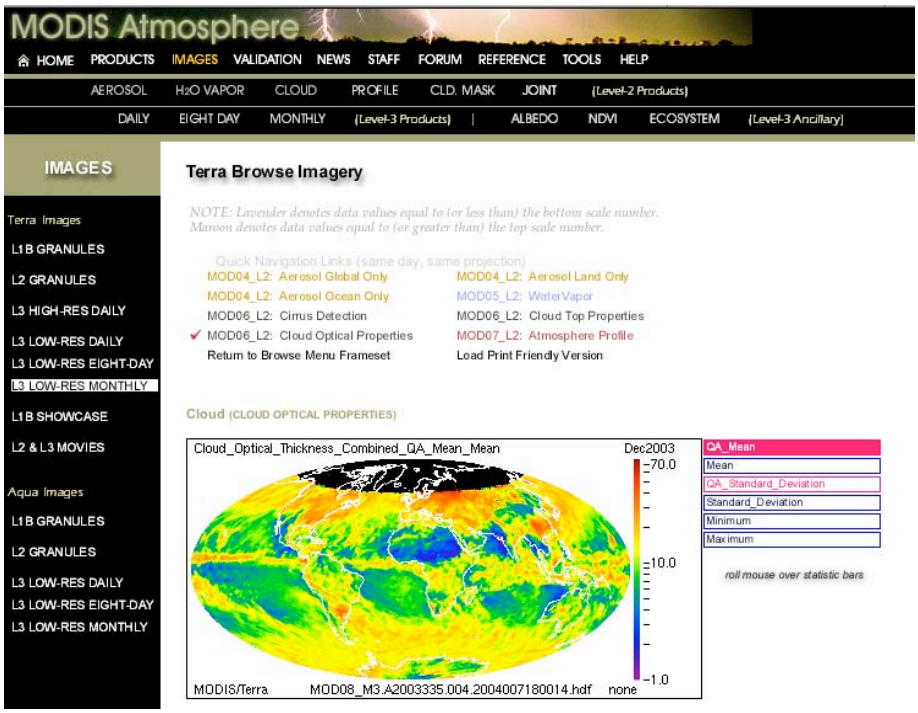

Figure 11. Level-3 daily browse images of cloud optical thickness for Terra on December 2003. In addition to the QA-weighted mean optical properties, one can select the minimum, maximum, standard deviation, and mean and standard deviation using java rollovers.

then select the image below that corresponds to that UTC time. These thumbnails blow up when selected to show a higher resolution version of the granule of interest.

In addition to the Level-1b browse images for all Terra and Aqua daytime granules, we also provide quicklook images of all Level-3 daily, eight day, monthly, and high-resolution (0.1° x 0.1°) images for both Terra and Aqua. Figure 11 shows a screen shot of the Level-3 monthly quicklook images page of MODIS cloud optical properties derived from Terra data on December 2003. In addition to QA-weighted mean cloud optical properties, we also provide the minimum, maximum, QA-weighted standard deviation, and mean and standard deviation for each time period using roll-over java applets.

Finally, to enable a user to readily determine not only what data have been analyzed, but also the status of the version used to process these data, we provide a data availability calendar (cf. Figure 12). The color code of the entry by satellite and month denote the status of the validation (provisional yellow and validated at various stages in green). In addition, the red numbers on each of the entries reflect the PGE version number used to process the data. At the bottom of the table there is a red button that contains the details of the PGE version so a user can easily determine the nature of any changes or updates that have occurred in processing the data.

At the end of this contract, the MODIS atmosphere web site uses 131 GB of disk

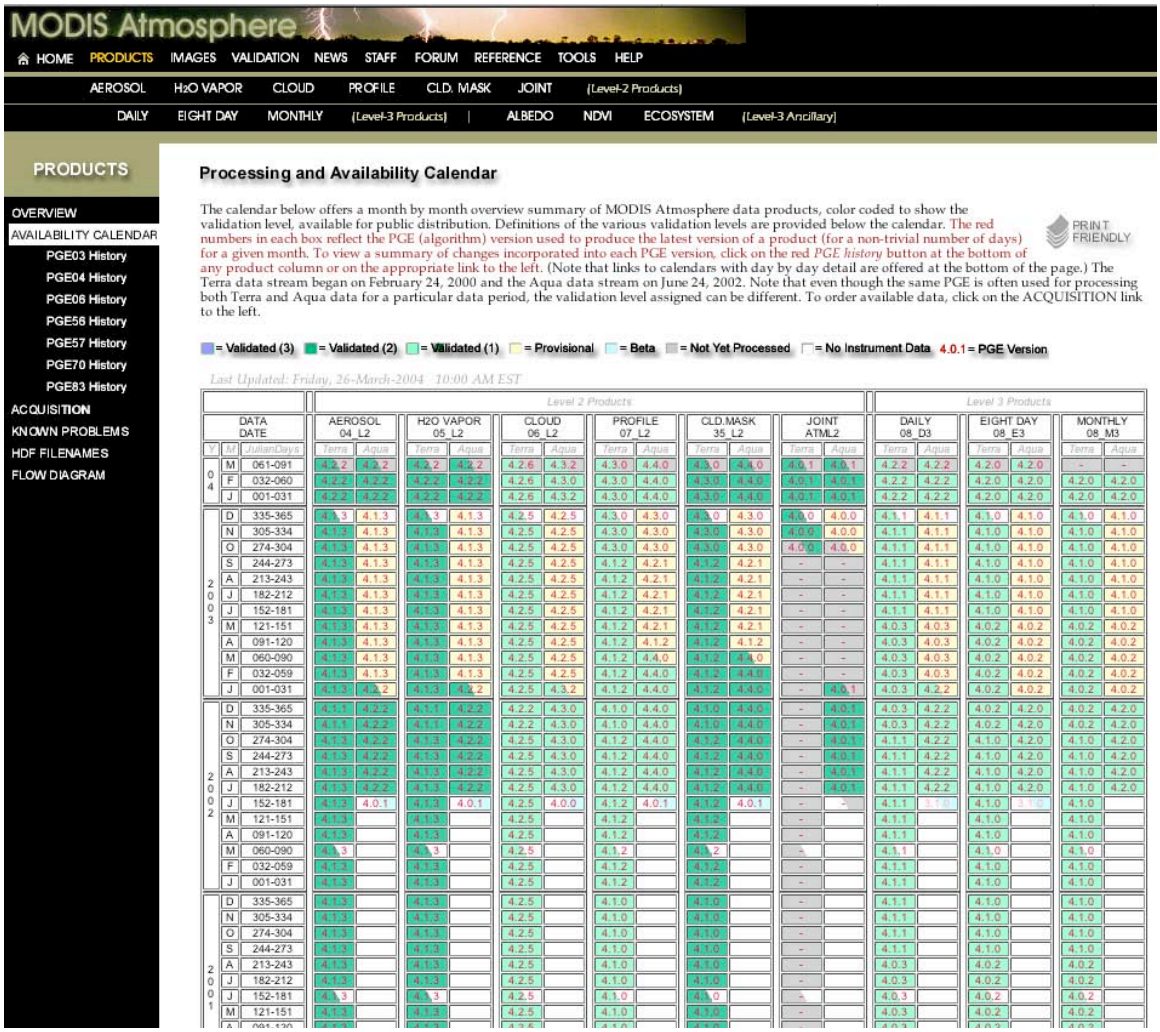

Figure 12. Data availability calendar for all MODIS atmosphere data products for both Terra and Aqua. The validation status is color coded, and the version used to produce the data is contained in the PGE version number (e.g., 4.3.2). A link to the PGE software changes and updates are contained in the red 'PGE details' at the bottom of the calendar.

space, and consists of 1.9 million files (images and html pages). This is a tremendous undertaking, but it provided for the benefit not only of the external scientific community wishing to find out the documentation, data production status, and imagery, but it is also vital for the algorithm developers in the MODIS atmosphere group to view the production and quality status of their algorithms.

B. Web Site Lessons Learned

- At the beginning of this contract period, the World Wide Web did not exist except on very few unix-based workstations. Its widespread growth and availability has greatly enhanced the ability to communicate algorithm details, documentation, visualization and data-access tools, and publications of note.

- Careful attention to web design and display is valuable for aiding comments and feedback from the broader scientific community on the quality and importance of the data products.

- An access point for data extraction and visualization tools, as well as data ordering tools, makes acceptance and use by the scientific community much more rapid than would otherwise be possible.

V. MODIS-related Field Campaigns and Validation Efforts

A. Level-2 Related Validation Activities

The cloud retrieval group has developed and utilized airborne scanning radiometers for algorithm development and field validation activities. These have included the development and utilization of the Cloud Absorption Radiometer (CAR; King et al. 1986) and MODIS Airborne Simulator (MAS; King et al. 1996). The MAS was developed under this contract for the express purpose of obtaining real airborne multispectral images of the Earth's atmosphere and surface to aid in the development of algorithm for the processing of MODIS data, once launched.

The cloud retrieval group has been involved in numerous field campaigns during the duration of this contract, including the following (*MAS + ER-2 flight scientist role, &CAR instrument studies). These campaigns have consisted of the following experiments:

ASTEX* (North Atlantic Sc clouds, summer 1992)
SCAR-A (Western Atlantic, summer 1993)
MAST* (Ship Tracks off coast of California, summer 1994)
ARMCAS* (Arctic clouds, summer 1995)
SCAR-B (Fires/smoke in Amazon basin, summer 1995)
SUCCESS (Cirrus clouds over Midwestern U.S., spring 1996)
TARFOX (Aerosols off east coast of U.S., summer 1996)
FIRE-ACE/SHEBA*,& (Arctic cloud studies, summer 1998)
SAFARI 2000*,& (Fire/smoke in southern Africa, Namibian stratocumulus clouds, summer 2000)
CLAMS& (Chesapeake Bay, summer 2001)
CRYSTAL-FACE* (Deep convection in vicinity of southern Florida, summer 2002)

These studies have fallen into several distinct scientific investigations, examples of which are given below.

B. Bidirectional Reflectance Properties of Clouds and Surfaces

The cloud retrieval group has developed and utilized the Airborne Cloud Absorption Radiometer to acquire BRDF measurements of the ocean, sea ice, snow,

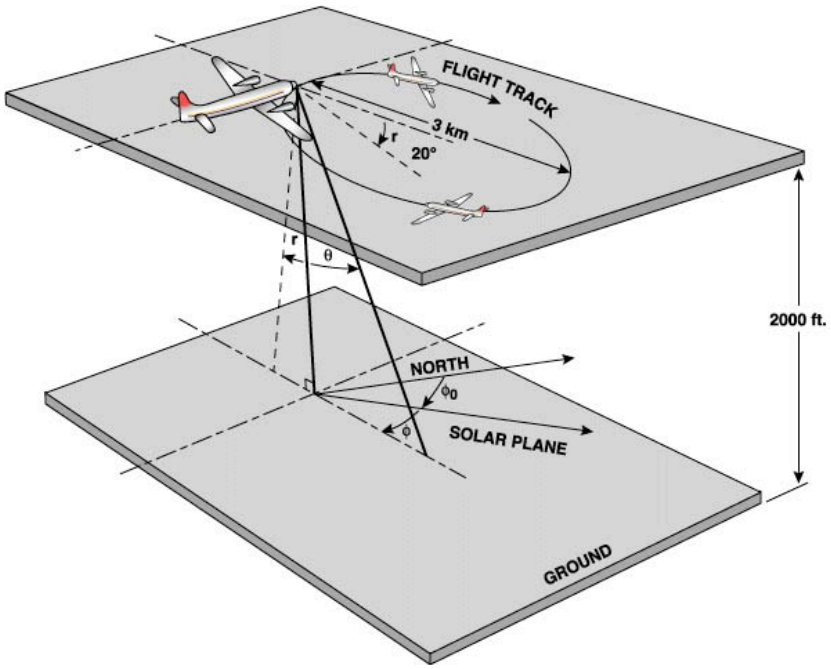

Figure 13. Schematic illustration of a clockwise circular flight track for measuring surface bidirectional reflectance from nadir to the horizon as we as much of the transmittance pattern from near zenith to the horizon (adapted from King 1992).

tundra, savanna (cerrado, mopane, miombo), smoke, vegetation, desert (Saudi Arabia, salt pans in Botswana and Namibia), and clouds between 0.5 and 2.3 μm. These measurements involve flights onboard the University of Washington C-131A or CV-580, and date from observations over the Kuwait oil fire smoke and nearby Saudi Arabian Desert and Persian Gulf in 1991 (King 1992), and extend to the more recent CLAMS experiment over ocean surfaces with sunglint (Gatebe et al. 2004).

Figure 13 shows a typical flight pattern whereby the aircraft, with the CAR in the nosecone, flight a clockwise circular pattern above the surface or cloud repeatedly, drifting with the wind, and scan the underlying surface and much or the transmitted solar radiation from above, and made radiometric observations about every 1° in azimuth and better than 1° in zenith angle with the CAR's instantaneous field-of-view of 1°. Often, multiple circular orbits are averaged together to smooth out the reflected solar radiation signal.

Figure 14 shows selected examples of the bidirectional reflectance observed over selected terrestrial surfaces, including Namibian stratus with a rainbow and glory the Etosha Pan, Namibia, and savanna vegetation at Skukuza, South Africa (Gatebe et al. 2003), and ocean reflectance with sunglint off the Virginia coast in the western Atlantic (Gatebe et al. 2004).

C. Remote Sensing of Cloud Optical and Microphysical Properties

The cloud retrieval group developed the MODIS Airborne Simulator in collabo-

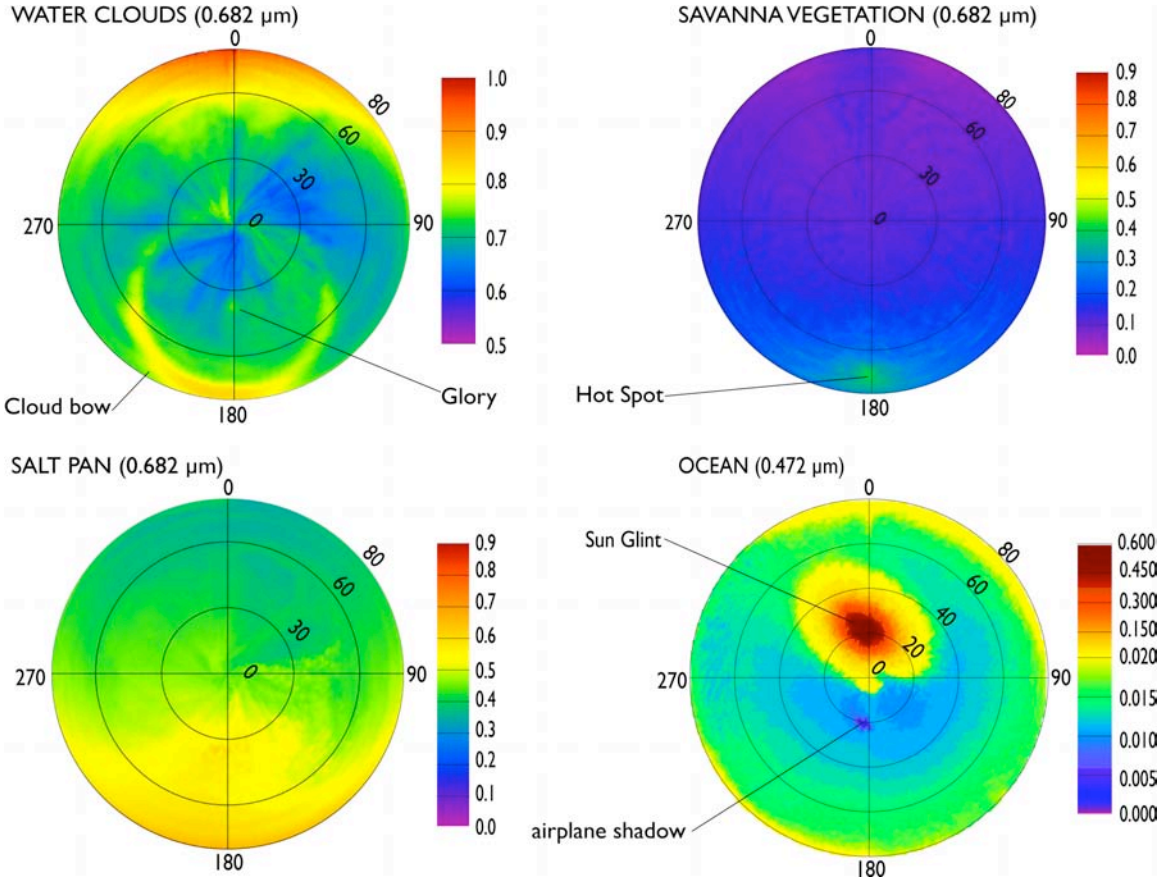

Figure 14. Bidirectional reflectance of various natural surfaces observed by the CAR mounted on the University of Washington CV-580 research aircraft. These observations have all been atmospherically corrected, and include Namibian stratus clouds and the Etosha salt pans of Africa, savanna vegetation in South Africa, and ocean reflectance with sunglint over the western Atlantic Ocean off Virginia, US.

ration with the University of Wisconsin (Paul Menzel, Chris Moeller, Liam Gumley) and Ames Research Center (Jeff Myers, Pat Grant, Mike Fitzgerald), which first flew, in an abbreviation form, on the NASA ER-2 aircraft in 1991 during FIRE II cirrus experiment (King et al. 1996).

Three airborne field campaigns have been especially beneficial for testing and developing algorithms and satellite validation strategies.

1. FIRE-ACE

The FIRE Arctic Cloud Experiment, or FIRE-ACE, was conducted in the Arctic between April and July 1998, with the component of interest to the MODIS science team being confined to a 5 week period consisting of the University of Washington CV-580 along with a 3 week period of high-altitude ER-2 overflights (cf. Curry et al. 2000 for further details). In addition, the ER-2 participated as the upper level aircraft from May 18-June 6, with the MAS, CLS, HIS, a multispectral along-track scanning radiometer (AirMISR), a Microwave Imaging Radiometer

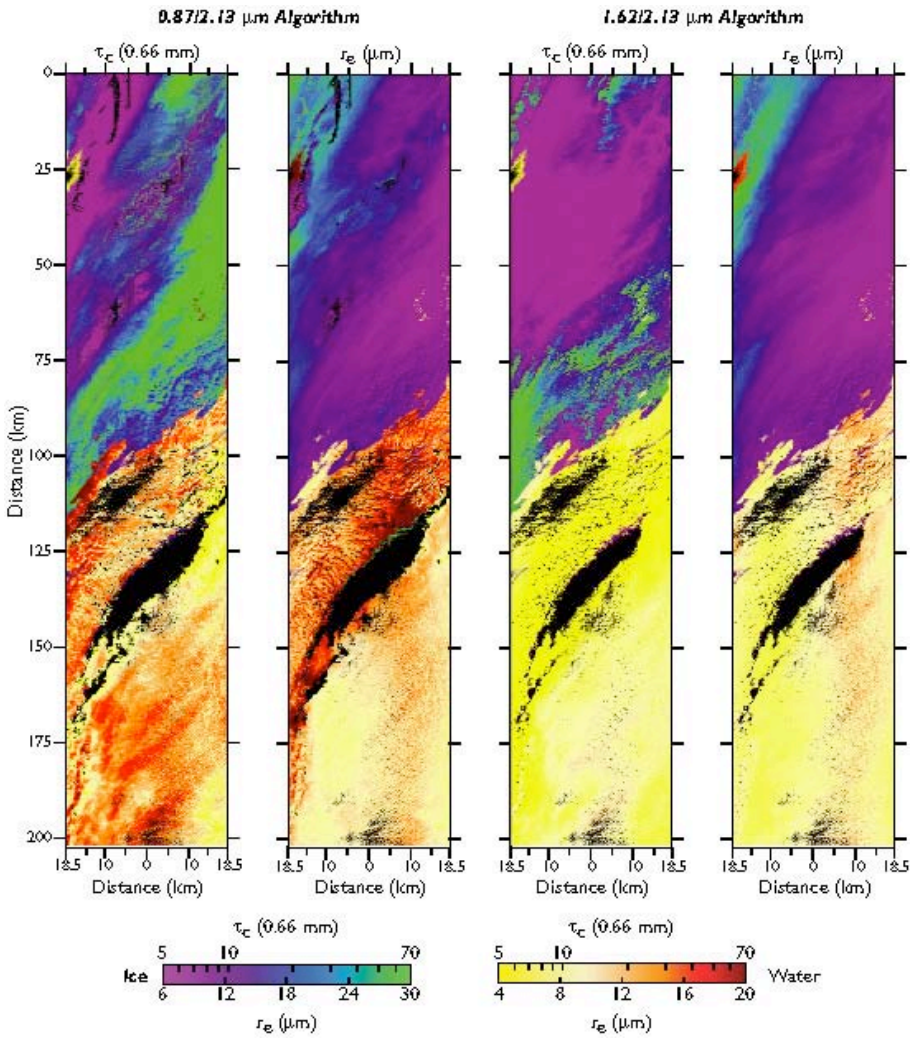

Figure 15. Cloud optical thickness and effective radius derived from MAS retrievals for stratiform water and ice cloud over a sea ice surface (north of Barrow AK). Two versions (different band combinations) of the retrieval algorithm are shown (King et al. 2004).

(MIR), a Solar Spectral Flux Radiometer (SSFR), and an Advanced Microwave Precipitation Radiometer (AMPR). All of these ER-2 sensors are of interest to Goddard Space Flight Center (Michael King, Si-Chee Tsay, Steve Platnick), as well as the CAR on the CV-580 and numerous in situ microphysics probes that were invaluable in accessing the accuracy of cloud retrievals of the microphysical and radiative properties of Arctic stratus clouds over a bright (sea ice) surface.

This valuable data set was used by the University of Wisconsin group for testing the cloud mask algorithm for readiness at-launch. The suite of measurements made during FIRE ACE and subsequent collaborative analyses provide a means to validate current and future satellite remote sensing methods and products (cloud optical thickness τ_c, effective radius r_e, single scattering albedo ω_0), the cloud mask, and precipitable water.

Figure 15 shows retrievals of cloud optical thickness and effective radius derived

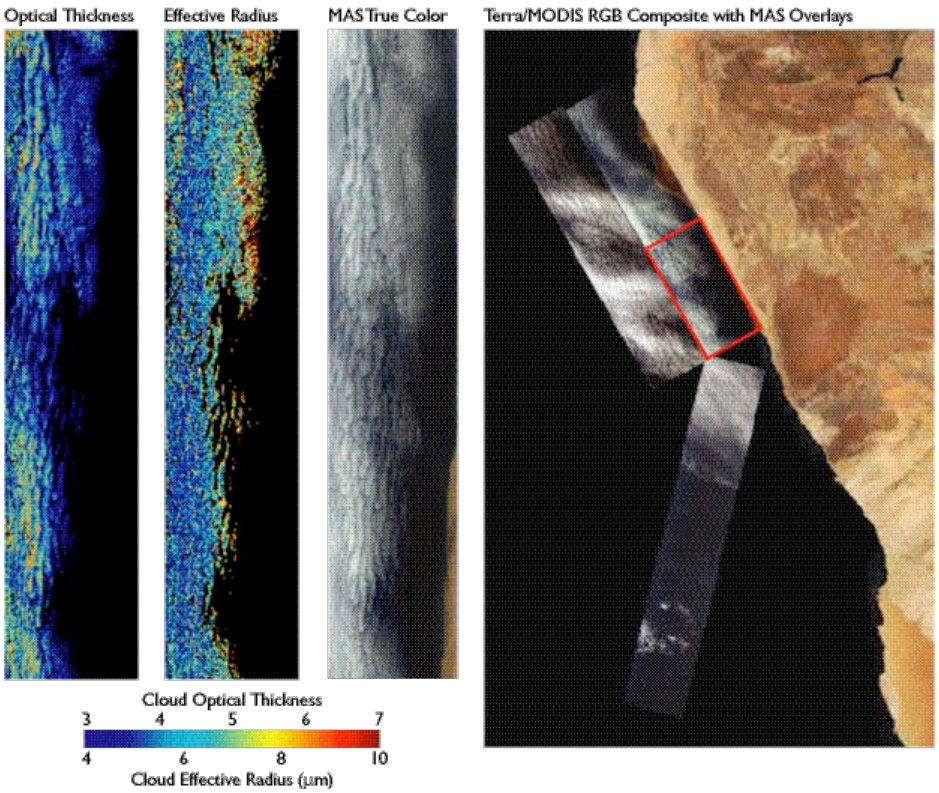

Figure 16. MAS retrievals of cloud optical thickness and effective radius for part of one ER-2 flight line along the coast of Namibia on 11 September 2000. Analyses such as these will be compared with collocated MODIS analyses and *in situ* microphysical retrievals.

using two different retrieval algorithms, the pair on the left being the closest to the currently operating MODIS retrieval algorithm, and the pair on the right a new algorithm, first developed based on airborne measurements obtained by the MAS during FIRE-ACE (Platnick et al. 2001), for use when the underlying surface has very high surface albedo in the visible wavelength region, as it does over sea ice.

2. SAFARI 2000

ER-2 and *in situ* microphysical measurements were obtained throughout southern Africa during SAFARI 2000 (King et al. 2003b) of biomass burning aerosol, land surface, fires, and marine stratocumulus clouds off the west coast of Namibia. It served as the first MODIS validation activity for water cloud optical and microphysical retrievals after the launch of Terra.

Figure 16 illustrates an example of the determination of cloud optical thickness and effective radius using the research 1.6/2.1 μm retrieval algorithm described by Platnick et al. (2001) as applied to MAS data collected during SAFARI 2000 off Namibia. On this day the Terra satellite overflew the NNE/SSW flight track shown on the MODIS image on the right, but the vast majority of this flight track was clear sky. The *in situ* microphysical measurements were obtained by the United Kingdom C-130, which was making repeated vertical profiles through the

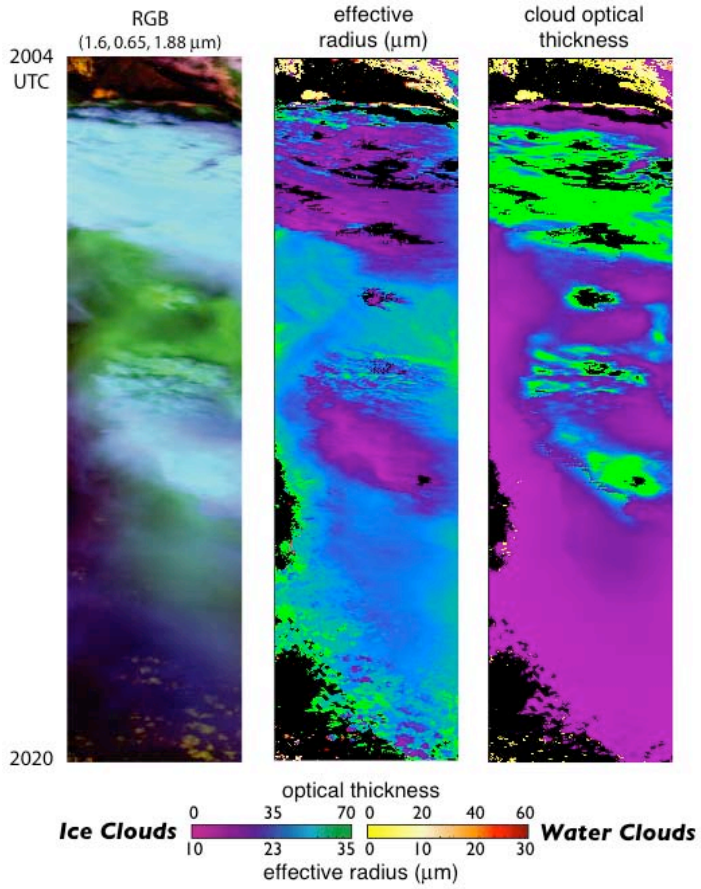

Figure 17. A CRYSTAL-FACE MAS retrieval from July 23, 2002. Convective cores (larger optical thickness) in the middle and top of the image are correlated with small particle sizes. Failed retrievals (black regions) in the optically thick parts of the cloud correspond to reflectances outside the library space.

cloud layer along the flight track that was analyzed in this figure. This was a relatively thin cloud for which the MAS retrieval yielded a mean cloud optical thickness $\tau_c = 3.8 \pm 0.85$ and a cloud effective radius $r_e = 5.9 \pm 1.3$ μm.

Analyses such as these, using data already acquired from airborne field validation campaigns like SAFARI 2000, have been examined to intercompare (i) MODIS retrievals with *in situ* microphysical retrievals, (ii) MODIS and MAS retrievals using nearly the same algorithm, and (iii) MAS retrievals with *in situ* microphysical retrievals. The different spatial resolution of MAS (50 m at nadir) contrasts greatly with the satellite retrievals using 1 km pixels, so point-by-point intercomparisons are not practical.

3. CRYSTAL-FACE

The CRYSTAL-FACE field campaign during July 2002 sought to understand the life cycle and radiative properties of anvil cirrus and involved six aircraft, 2 ground sites, and several hundred scientists. It served as the first MODIS validation activity for ice cloud optical and microphysical retrievals.

The initial work with the CRYSTAL-FACE MAS data set focused on assessment of the cloud mask and thermodynamic phase algorithms. As part of this contract, a Fortran 90 version of the MODIS retrieval code for use in processing MAS. A number of selected flight tracks of MAS data from the CRYSTAL-FACE were processed with the MAS cloud mask, thermodynamic phase, and optical thickness and effective radius code. Figure 17 shows an example of this retrieval for July 23, 2002.

MODIS images from both Terra and Aqua have been processed and visualized for all flight days and distributed to interested investigators on the CRYSTAL-FACE science team.

VI. Publications

A. Published

1. Arnold, G. T., S. C. Tsay, M. D. King, J. Y. Li, and P. F. Soulen, 2002: Airborne spectral measurements of surface-atmosphere anisotropy for Arctic sea ice and tundra. *Int. J. Remote Sens.*, **23**, 3763–3781.

2. Baum, B. A., P. F. Soulen, K. I. Strabala, M. D. King, S. A. Ackerman, W. P. Menzel, and P. Yang, 2000: Remote sensing of cloud properties using MODIS Airborne Simulator imagery during SUCCESS. II: Cloud thermodynamic phase. *J. Geophys. Res.*, **105**, 1781–11792.

3. Curry, J. A. P. V. Hobbs, M. D. King, D. A. Randall, P. Minnis, G. A. Isaac, J. O. Pinto, T. Uttal, A. Bucholtz, D. G. Cripe, H. Gerber, C. W. Fairall, T. J. Garrett, J. Hudson, J. M. Intrieri, C. Jakob, T. Jensen, P. Lawson, D. Marcotte, L. Nguyen, P. Pilewskie, A. Rangno, D. C. Rodgers, K. B. Strawbridge, F. P. J. Valero, A. G. Williams, and D. Wylie, 2000: FIRE Arctic Clouds Experiment. *Bull. Amer. Meteor. Soc.*, **81**, 5–30.

4. Gatebe, C. K., M. D. King, S. Platnick, G. T. Arnold, E. F. Vermote, and B. Schmid, 2003: Airborne spectral measurements of surface-atmosphere anisotropy for several surfaces and ecosystems over southern Africa. *J. Geophys. Res.*, **108**, 8489, doi:10.1029/2002JD002397.

5. Gatebe, C. K., M. D. King, S. C. Tsay, Q. Ji, G. T. Arnold, and J. Y. Li, 2001: Sensitivity of off-nadir zenith angles to correlation between visible and near-infrared reflectance for use in remote sensing of aerosol over land. *IEEE Trans. Geosci. Remote Sens.*, **39**, 805–819.

6. Kaufman, Y. J., D. Tanré, H. R. Gordon, T. Nakajima, J. Lenoble, R. Frouin, H. Grassl, B. M. Herman, M. D. King, and P. M. Teillet, 1997: Passive remote sensing of tropospheric aerosol and atmospheric correction for the aerosol effect. *J. Geophys. Res.*, **102**, 16815–16830.

7. Kaufman, Y. J., P. V. Hobbs, V. W. J. H. Kirchhoff, P. Artaxo, L. A. Remer, B. N. Holben, M. D. King, D. E. Ward, E. M. Prins, K. M. Longo, L. F. Mattos, C. A. Nobre, J. D. Spinhirne, Q. Ji, A. M. Thompson, J. F. Gleason, S. A. Christopher, and S. C. Tsay, 1998: Smoke, Clouds, and Radiation—Brazil (SCAR-B) experiment. *J. Geophys. Res*., **103**, 31783–31808.

8. King, M. D., and D. D. Herring, 2000: Monitoring Earth's vital signs. *Sci. Amer*., **282**, 72–77.

9. King, M. D., and D. D. Herring, 2002: Research satellites (atmospheric sciences). *Encyclopedia of Atmospheric Sciences*, J. R. Holton, J. A. Pyle, and J. A. Curry, Eds., Academic Press, 2038–2047.

10. King, M. D., D. D. Herring, and D. J. Diner, 1995: The Earth Observing System (EOS): A space-based program for assessing mankind's impact on the global environment. *Opt. Photon. News*, **6**, 34–39.

11. King, M. D., Y. J. Kaufman, W. P. Menzel, and D. Tanré, 1992: Remote sensing of cloud, aerosol, and water vapor properties from the Moderate Resolution Imaging Spectrometer (MODIS). *IEEE Trans. Geosci. Remote Sens*., **30**, 2–27.

12. King, M. D., Y. J. Kaufman, D. Tanré, and T. Nakajima, 1999: Remote sensing of tropospheric aerosols from space: Past, present, and future. *Bull. Amer. Meteor. Soc*., **80**, 2229–2259.

13. King, M. D., W. P. Menzel, P. S. Grant, J. S. Myers, G. T. Arnold, S. E. Platnick, L. E. Gumley, S. C. Tsay, C. C. Moeller, M. Fitzgerald, K. S. Brown, and F. G. Osterwisch, 1996: Airborne scanning spectrometer for remote sensing of cloud, aerosol, water vapor and surface properties. *J. Atmos. Oceanic Technol*., **13**, 777–794.

14. King, M. D., W. P. Menzel, Y. J. Kaufman, D. Tanré, B. C. Gao, S. Platnick, S. A. Ackerman, L. A. Remer, R. Pincus, and P. A. Hubanks, 2003: Cloud and aerosol properties, precipitable water, and profiles of temperature and humidity from MODIS. *IEEE Trans. Geosci. Remote Sens.*, **41**, 442–458.

15. King, M. D., S. Platnick, C. C. Moeller, H. E. Revercomb and D. A. Chu, 2003: Remote sensing of smoke, land and clouds from the NASA ER-2 during SAFARI 2000. *J. Geophys. Res.*, **108**, 8502, doi:10.1029/2002JD003207.

16. King, M. D., S. C. Tsay, S. A. Ackerman, and N. F. Larsen, 1998: Discriminating heavy aerosol, clouds, and fires during SCAR-B: Application of airborne multispectral MAS data. *J. Geophys. Res*., **103**, 31989–31999.

17. Marchand, R. T., T. P. Ackerman, M. D. King, C. Moroney, R., Davies, J. P. Muller, and H. Gerber, 2001: Multiangle observations of arctic stratus clouds from FIRE ACE: June 3, 1998, case study. *J. Geophys. Res.*, **106**, 15201–15214.

18. Nakajima, T., and M. D. King, 1992: Asymptotic theory for optically thick layers: Application to the discrete ordinates method. *Appl. Opt.*, **31**, 7669–7683.

19. Ou, S. C., K. N. Liou, M. D. King, and S. C. Tsay, 1999: Remote sensing of cirrus cloud parameters based on a 0.63-3.7 μm radiance correlation technique applied to AVHRR data. *Geophys. Res. Lett.*, **26**, 2437–2440.

20. Platnick, S., 2000: Vertical photon transport in cloud remote sensing problems. *J. Geophys. Res.*, **105**(D18), 22919–22935.

21. Platnick, S., 2001: A superposition technique for deriving photon scattering statistics in plane-parallel cloudy atmospheres. *J. Quant. Spectrosc. Radiat. Transfer*, **68**, 57–73.

22. Platnick, S., 2001: Approximations for horizontal transport in cloud remote sensing problems. *J. Quant. Spectrosc. Radiat. Transfer*, **68**, 75–99.

23. Platnick, S., M. D. King, S. A. Ackerman, W. P. Menzel, B. A. Baum, J. C. Riédi, and R. A. Frey, 2003: The MODIS cloud products: Algorithms and examples from Terra. *IEEE Trans. Geosci. Remote Sens.*, **41**, 459–473.

24. Platnick, S., J. Y. Li, M. D. King, H. Gerber, and P. V. Hobbs, 2001: A solar reflectance method for retrieving the optical thickness and droplet size of liquid water clouds over snow and ice surfaces. *J. Geophys. Res.*, **106**, 15185–15199.

25. Price, R. D., M. D. King, J. T. Dalton, K. S. Pedelty, P. E. Ardanuy, and M. K. Hobish, 1994: Earth science data for all: EOS and the EOS Data and Information System. *Photogramm. Eng. Remote Sens.*, **60**, 277–285.

26. Rolland, P., K. N. Liou, M. D. King, S. C. Tsay, and G. M. McFarquhar, 2000: Remote sensing of optical and microphysical properties of cirrus clouds using MODIS channels: Methodology and sensitivity to assumptions. *J. Geophys. Res.*, **105**, 11721–11738.

27. Soulen, P. F., M. D. King, S. C. Tsay, G. T. Arnold, and J. Y. Li, 2000: Airborne spectral measurements of surface-atmosphere anisotropy during the SCAR-A, Kuwait oil fire, and TARFOX experiments. *J. Geophys. Res.*, **105**, 10203–10218.

28. Swap, R. J., H. J. Annegarn, J. T. Suttles, J. Haywood, M. C. Helmlinger, C. Hely, P. V. Hobbs, B. N. Holben, J. Ji, M. D. King, T. Landmann, W. Maenhaut, L. Otter, B. Pak, S. J. Piketh, S. Platnick, J. Privette, D. Roy, A. M. Thompson, D. Ward, and R. Yokelson, 2002: The southern African regional science initiative (SAFARI 2000): Overview of the dry season field campaign. *S. African J. Sci.*, **98**, 125–130.

29. Swap, R. J., H. J. Annegarn, J. T. Suttles, M. D. King, S. Platnick, J. L. Privette

and R. J. Scholes, 2003: Africa burning: A thematic analysis of the Southern African Regional Science Initiative (SAFARI 2000). *J. Geophys. Res.*, **108**, 8465, doi:10.1029/2003JD003747.

30. Tsay, S. C., P. M. Gabriel, M. D. King, and G. L. Stephens, 1996: Spectral reflectance and atmospheric energetics in cirrus-like clouds. Part II: Applications of a Fourier-Riccati approach to radiative transfer. *J. Atmos. Sci.*, **53**, 3450–3467.

31. Tsay, S. C., M. D. King, G. T. Arnold, and J. Y. Li, 1998: Airborne spectral measurements of surface anisotropy during SCAR-B. *J. Geophys. Res.*, **103**, 31943–31953.

32. Wang, M., and M. D. King, 1997: Correction of Rayleigh scattering effects in cloud optical thickness retrievals. *J. Geophys. Res.*, **102**, 25915–25926.

33. Wielicki, B. A., R. D. Cess, M. D. King, D. A. Randall, and E. F. Harrison, 1995: Mission to Planet Earth: Role of clouds and radiation in climate. *Bull. Amer. Meteor. Soc.*, **76**, 2125–2153.

34. Yang, P., B. C. Gao, W. J. Wiscombe, M. I. Mishchenko, S. E. Platnick, H. L. Huang, B. A. Baum, Y. X. Hu, D. M. Winker, S. C. Tsay, S. K. Park, 2002: Inherent and apparent scattering properties of coated or uncoated spheres embedded in an absorbing medium. *Appl. Opt.*, **41**, 2740–2759.

B. Submitted or Accepted for Publication

1. Baum, B. A., and S. Platnick, 2004: Introduction to MODIS cloud product. *Remote Sensing*, Springer, J. J. Qu, W. Gao, M. Kafatos, R. Murphy, V. Salomonson, Eds. (submitted).

2. Gatebe, C. K., M. D. King, A. I. Lyapustin, G. T. Arnold, and J. Redemann, 2004: Airborne spectral measurements of ocean directional reflectance. Submitted to *J. Atmos. Sci.*

3. King, M. D., S. Platnick, P. Yang, G. T. Arnold, M. A. Gray, J. C. Riédi, S. A. Ackerman, and K. N. Liou, 2004: Remote sensing of liquid water and ice cloud optical thickness, and effective radius in the arctic: Application of airborne multispectral MAS data. *J. Atmos. Oceanic Technol.*, in press.

4. Mace, G. G., Y. Zhang, S. Platnick, M. D. King, P. Minnis, and P. Yang, 2004: Evaluation of cirrus cloud properties derived from MODIS radiances using cloud properties derived from ground-based data collected at the ARM SGP site. *J. Appl. Meteor.*, in press.

5. Moody, E. G., M. D. King, S., Platnick, C. B. Schaaf, and F. Gao, 2004: Spatially complete surface albedo datasets: Value-added products derived from Terra

MODIS land products. Submitted to *IEEE Trans. Geosci. Remote Sens*.

C. *Other Publications*

1. Chu, A., K. Strabala, S. Platnick, E. Moody, M. King, S. Matoo, R. Hucek and W. Ridgway, 2000: MODIS Atmosphere QA Plan, 23 pp.

2. King, M. D., Y. J. Kaufman, W. P. Menzel, D. Tanré, B. C. Gao et al., 2003: MODIS Atmosphere Validation Plan, 49 pp.

3. King, M. D., S. C. Tsay, S. E. Platnick, M. Wang and K. N. Liou, 1997: *Cloud Retrieval: Algorithms for MODIS: Optical Thickness, Effective Particle Radius, and Thermodynamic Phase*. Algorithm Theoretical Basis Document ATBD-MOD-05, Goddard Space Flight Center, 79 pp. (available at modis-atmos.gsfc.nasa.gov/reference_atbd.html).

4. Pinker, R. T., H. Wang, M. D. King, and S. Platnick, 2003: A first view of global radiative fluxes from MODIS. *GEWEX News*, **13**, No. 4, November 2003.

VII. Awards

1. Michael King was elected *Fellow*, *American Meteorological Society* (1990).

2. Michael King received the *NASA Exceptional Scientific Achievement Medal* (1992)

3. Michael King received the *Transactions Prize Paper Award*, *IEEE Geoscience and Remote Sensing Society* (1993)

4. Michael King received an *honorary D.Sc.*, *Colorado College* (1995)

5. Michael King received the *Verner E. Suomi Award*, *American Meteorological Society* (2000)

6. Michael King received the *William Nordberg Memorial Award for Earth Sciences*, the highest award of the Goddard space Flight Center for Achievement in research in Earth systems science (2001).

7. Michael King received the *NASA Outstanding Leadership Medal* (2001)

8. Michael King was elected to the *National Academy of Engineering* (2003)

9. Michael King was elected *Senior Member*, *Institute of Electrical and Electronics Engineers* (2003).

10. Steven Platnick and Michael King received the *NASA Group Achievement Award* for Outstanding Teamwork, Earth Observing System (EOS) Aqua Mis-

sion Team (2003)

11. Steven Platnick and Michael King received the *NASA Group Achievement Award* for SAFARI 2000 International Leadership Team (2003)

VIII. Web sites

The MODIS Atmosphere, MAS, and CAR web sites were developed and maintained by this contract, and can be found at:

modis-atmos.gsfc.nasa.gov
mas.arc.nasa.gov
car.gsfc.nasa.gov

IX. References

Ackerman, S. A., K. I. Strabala, W. P. Menzel, R. A. Frey, C. C. Moeller, and L. E. Gumley, 1998: Discriminating clear-sky from clouds with MODIS. *J. Geophys. Res.*, **103**, 32141–32158.

Baum, B. A., D. P. Kratz, P. Yang, S. Ou, Y. X. Hu, P. F. Soulen and S. Ch Tsay, 2000a: Remote sensing of cloud properties using MODIS Airborne Simulator imagery during SUCCESS. I. Data and models. *J. Geophys. Res.*, **105**, 11767–11780.

Baum, B. A., P. F. Soulen, K. I. Strabala, M. D. King, S. A. Ackerman, W. P. Menzel, and P. Yang, 2000b: Remote sensing of cloud properties using MODIS Airborne Simulator imagery during SUCCESS. II: Cloud thermodynamic phase. *J. Geophys. Res.*, **105**, 11781–11792.

Berk, A, L. S. Bernstein, G. P. Anderson, P. K. Acharya, D. C. Robertson, J. H. Chetwynd, and S. M. Adler-Golden, 1998: MODTRAN cloud and multiple scattering upgrades with application to AVIRIS. *Remote Sens. Environ.*, **65**, 367–375.

Curry, J. A. P. V. Hobbs, M. D. King, D. A. Randall, P. Minnis, G. A. Isaac, J. O. Pinto, T. Uttal, A. Bucholtz, D. G. Cripe, H. Gerber, C. W. Fairall, T. J. Garrett, J. Hudson, J. M. Intrieri, C. Jakob, T. Jensen, P. Lawson, D. Marcotte, L. Nguyen, P. Pilewskie, A. Rangno, D. C. Rodgers, K. B. Strawbridge, F. P. J. Valero, A. G. Williams, and D. Wylie, 2000: FIRE Arctic Clouds Experiment. *Bull. Amer. Meteor. Soc.*, **81**, 5–30.

Gatebe, C. K., M. D. King, A. I. Lyapustin, G. T. Arnold, and J. Redemann, 2004: Airborne spectral measurements of ocean directional reflectance. Submitted to *J. Atmos. Sci.*

Gatebe, C. K., M. D. King, S. Platnick, G. T. Arnold, E. F. Vermote, and B. Schmid, 2003: Airborne spectral measurements of surface-atmosphere anisotropy for

several surfaces and ecosystems over southern Africa. *J. Geophys. Res.*, **108**, 8489, doi:10.1029/2002JD002397.

King, M. D., 1992: Directional and spectral reflectance of the Kuwait oil-fire smoke. *J. Geophys. Res.*, **97**, 14545–14549.

King, M. D., M. G. Strange, P. Leone, and L. R. Blaine, 1986: Multiwavelength scanning radiometer for airborne measurements of scattered radiation within clouds. *J. Atmos. Oceanic Technol.*, **3**, 513–522.

King, M. D., S. C. Tsay, S. A. Ackerman and N. F. Larsen, 1998: Discriminating heavy aerosol, clouds, and fires during SCAR-B: Application of airborne multispectral MAS data. *J. Geophys. Res.*, **103**, 31989–32000.

King, M. D., W. P. Menzel, Y. J. Kaufman, D. Tanré, B. C. Gao, S. Platnick, S. A. Ackerman, L. A. Remer, R. Pincus, and P. A. Hubanks, 2003a: Cloud and aerosol properties, precipitable water, and profiles of temperature and humidity from MODIS. *IEEE Trans. Geosci. Remote Sens.*, **41**, 442–458.

King, M. D., S. Platnick, C. C. Moeller, H. E. Revercomb and D. A. Chu, 2003b: Remote sensing of smoke, land and clouds from the NASA ER-2 during SAFARI 2000. *J. Geophys. Res.*, **108**, 8502, doi:10.1029/2002JD003207.

King, M. D., W. P. Menzel, P. S. Grant, J. S. Myers, G. T. Arnold, S. E. Platnick, L. E. Gumley, S. C. Tsay, C. C. Moeller, M. Fitzgerald, K. S. Brown, and F. G. Osterwisch, 1996: Airborne scanning spectrometer for remote sensing of cloud, aerosol, water vapor and surface properties. *J. Atmos. Oceanic Technol.*, **13**, 777–794.

King, M. D., S. Platnick, P. Yang, G. T. Arnold, M. A. Gray, J. C. Riédi, S. A. Ackerman, and K. N. Liou, 2004: Remote sensing of liquid water and ice cloud optical thickness, and effective radius in the arctic: Application of airborne multispectral MAS data. *J. Atmos. Oceanic Technol.*, in press.

Menzel, W. P., B. A. Baum, K. I. Strabala, and R. A. Frey, 2002: *Cloud Top Properties and Cloud Phase Algorithm Theoretical Basis Document*. Algorithm Theoretical Basis Document ATBD-MOD-04, Goddard Space Flight Center, 61 pp. (available at modis-atmos.gsfc.nasa.gov/reference_atbd.html).

Moody, E. G., M. D. King, S., Platnick, C. B. Schaaf, and F. Gao, 2004: Spatially complete surface albedo datasets: Value-added products derived from Terra MODIS land products. Submitted to *IEEE Trans. Geosci. Remote Sens*.

Nakajima, T., and M. D. King, 1990: Determination of the optical thickness and effective particle radius of clouds from reflected solar radiation measurements. Part I: Theory. *J. Atmos. Sci.*, **47**, 1878–1893.

Platnick, S., J. Y. Li, M. D. King, H. Gerber and P. V. Hobbs, 2001: A solar reflectance method for retrieving cloud optical thickness and droplet size over snow and ice surfaces. *J. Geophys. Res.*, **106**, 15185–15199.

Strabala, K. I., S. A. Ackerman, and W. P. Menzel, 1994: Cloud properties inferred from 8-12 μm data. *J. Appl. Meteor.*, **2**, 212–229.

Wang, M., and M. D. King, 1997: Correction of Rayleigh scattering effects in cloud optical thickness retrievals. *J. Geophys. Res.*, **102**, 25915-25926.